Transformation of C_{60} fullerene aggregates suspended and weathered under realistic environmental conditions

Josep Sanchís[1,†], Yann Aminot[2,†], Esteban Abad[1], Awadhesh N. Jha[2], James W. Readman[2,3], Marinella Farré[1,*]

[1] Water and Soil Quality Research Group, Institute of Environmental Assessment and Water Research (IDAEA-CSIC), C/Jordi Girona, 18-26, 08034, Barcelona, Catalonia, Spain.

[2] Biogeochemistry Research Centre, Plymouth University, Plymouth, PL4 8AA, UK.

[3] Plymouth Marine Laboratory, Prospect Place, The Hoe, Plymouth, PL1 3DH, UK

[†] Both authors contributed equally to this work.

[*] *Corresponding author*: Tel. +34 93 400 61 00 E-mail: mfuqam@cid.csic.es (Marinella Farré)

This is the author's accepted manuscript. The final published version of this work (the version of record) is published by Elsevier in Carbon on 24-11-2017 available at: https://doi.org/10.1016/j.carbon.2017.11.060 .This work is made available online in accordance with the publisher's policies. Please refer to any applicable terms of use of the publisher.

Abstract

The occurrence, fate and behaviour of carbon nanomaterials in the aquatic environment are dominated by their functionalization, association with organic material and aggregation behaviour. In particular, the degradation of fullerene aggregates in the aquatic environment is a primary influence on their mobility, sorption potential and toxicity. However, the degradation and kinetics of water suspensions of fullerenes remain poorly understood.

In the present work, first, an analytical method based on liquid chromatography and high-resolution mass spectrometry (LC-HRMS) for the determination of C_{60} fullerene and their environmental transformation products was developed. Secondly, a series of C_{60} fullerene water suspensions were degraded under relevant environmental conditions, controlling the salinity, the humic substances content, the pH and the sunlight irradiation. Up to ten transformation products were tentatively identified, including epoxides and dimers with two C_{60} units linked *via* one or two adjacent furane-like rings. Fullerenols were not observed under these environmentally relevant conditions.

The kinetics of generation of each transformation product were studied with and without simulated sunlight conditions. The ionic strength of the media, its pH and the humic substances content were observed to modulate the kinetics of generation.

1. Introduction

Since its discovery [1], C_{60} fullerene stands as one of the most deeply studied carbon-based nanomaterial. Nowadays, C_{60} fullerene and its derivatives have been proposed for use in medical applications [2, 3], in analytical chemistry [4, 5], in microelectronics components [6, 7], in solar cells' bulk hetero-junctions[8, 9] and as a component of a wide diversity of nanocomposites [10, 11]. In addition, fullerenes, together with other carbon nanomaterials, may be generated in highly energetic events of either natural or anthropogenic nature, including lightning discharges [12], meteorite (chondrite) impacts [13, 14], forest fires [15, 16], candles [17] and car engines [18]. The last consequence of all of these processes is the emission of fullerenes into the environment [19-26], where they are distributed amongst its different compartments.

The analysis of fullerenes in the environment is a relatively recent topic. From an analytical perspective, their analysis is challenging because of their extremely low environmental levels [27], the need for specific instrumentation, and their hydrophobicity. Besides, mass spectrometric analysis of fullerenes has some unique challenges: low ionization efficiencies are obtained with both electrospray ionisation (ESI) and atmospheric pressure chemical ionisation (APCI) sources and, in addition, the fragmentation of fullerenes by tandem mass spectrometers is virtually non-existent. Therefore, methods based on atmospheric pressure photoionization (APPI) sources and high resolution mass spectrometry (HRMS) are preferred [19, 21, 28]. Recent analytical approaches have allowed lower detection limits [29], and the occurrence of C_{60}s has been reported in rivers and ponds at low ng l^{-1} and sub-ng l^{-1} concentrations [21-24, 28]. Despite the extreme hydrophobicity of this molecule (log K_{OW}=6.67 [30]), C_{60} fullerene can be stabilized in water because (1) C_{60} is a strong sorbent material that is readily attached to suspended matter [31] and (2) fullerene molecules aggregate creating clusters [32] (termed herein as nC_{60}), the surfaces of which are surrounded by a "*stable spherical shell of interconnected water molecules*" [33].

It is well known that the colloidal behaviour of nC_{60} responds to the Derjaguin-Landau-Verwey-Overbeek (DLVO) model [34-36]. The stabilization of nC_{60} is attributed to repulsive van der Waals forces, but it is unclear to what extent the chemical functionalization of the aggregates' surface plays a role in the stability of nC_{60} in the real environment. For instance, it is known that UV irradiation induces chemical changes in

nC_{60} surfaces and enhances the stability of nC_{60} in water [37, 38]. This can be attributed to the excitation of C_{60} fullerene to singlet C_{60} ($^1C_{60}$), which in turn is converted into triplet C_{60} ($^3C_{60}$) via intersystem crossing (ISC), as described in equation 1.

$$^1C_{60} \xrightarrow{h\nu} {}^1C_{60}^* \xrightarrow{ISC} {}^3C_{60}^* \qquad \text{equation 1}$$

This mechanism was initially studied in benzene suspension by Arbogast *et al*. (1991) [39] and was later observed in aqueous suspension [40, 41]. Once generated, triple excited C_{60} undergoes several reactions, including self-quenching with ambient oxygen, which generates singlet oxygen and singlet C_{60} (equation 2); C_{60} oligomerization, via [2+2] cycloaddition (equation 3); and C_{60} functionalization, such as the formation of a variety of epoxides (equation 4) [42, 43].

$$^3C_{60} + {}^3O_2 \longrightarrow {}^1C_{60} + {}^1O_2 \qquad \text{equation 2}$$

$$m\ {}^3C_{60} \longrightarrow (C_{60})_m \qquad \text{equation 3}$$

$$^3C_{60} + \frac{x}{2}\ {}^1O_2 \longrightarrow C_{60}O_x\ , \quad x=1–5 \qquad \text{equation 4}$$

The production of these transformation products is dependent on two main factors: the type of irradiation and to the presence of ozone. With regards to the former, under strong irradiation conditions, reactions occur relatively quickly, whilst under natural sunlight they happen during weeks/months [44]. In addition, under harsh irradiation conditions, other transformation products have been observed, such as the C_{60} dicarbonyl [45], and even the breakdown of the fullerene carbon cage [46]. With regards to the presence of ozone, Fortner *et al* (2007) observed the high reactivity of nC_{60}, which resulted in the formation of oxidised transformation products with up to 29 oxygen atoms. Heymann *et al*. described the generation of the relatively stable [6,6]-closed C_{60} epoxide, upon ozonolysis, via decomposition of the intermediate [6,6]-closed C_{60} ozonide ($C_{60}O_3$) [47]. Murdianti *et al*. (2012) detected significant concentrations of the same [6,6]-closed C_{60} epoxide after the exposure to common ozone concentrations, under ambient air exposure [48].

The wide variety of (photo)transformation products and the influence of ambient factors on their generation underpin the need to faithfully reproduce realistic environmental conditions in order to unambiguously identify which C_{60} fullerene transformation products are generated in the real environment, to study their kinetics and, ultimately, to

study their occurrence in real samples. This topic has recently been addressed in air [49] and soil [50] matrices, but has not been systematically assessed in waters with different physicochemical properties.

In the present study, an analytical method based on high performance liquid chromatography coupled to high resolution mass spectrometry (HPLC-HRMS) was developed for the analysis of C_{60} transformation products. C_{60} was dispersed by long term stirring in artificial water media (containing environmentally relevant pH values, salt compositions and humic acid contents) and nC_{60} were exposed, under atmospheric condition, to controlled sunlight or dark conditions. The presence of environmentally relevant transformation products and their kinetics of formation were assessed.

2. Experimental section

2.1. Reagents and chemicals A standard of C_{60} fullerene (sublimed, 99.9 % purity; ref. 572500) was purchased from Sigma-Aldrich (Steinheim, Germany). ^{13}C-enriched C_{60} fullerene (>99 % purity; ref. MRL613), containing 45–55 % of ^{13}C atoms in each C_{60} molecule ($^{13}C_{27}{}^{12}C_{33}$–$^{13}C_{33}{}^{12}C_{27}$) was purchased from MER Corporation (Tucson, AZ, USA). The molecule $^{13}C_{30}{}^{12}C_{30}$ (m/z of its molecular radical anion, 750.1012) was used as an internal standard. Standards of humic acids (technical grade, reference 53680) and salts (including $CaCl_2$, $CaCl_2 \cdot 2H_2O$, H_3BO_3, KBr, KCl, $MgCl_2$, $MgCl_2 \cdot 6H_2O$, NaCl, NaF, $NaHCO_3$, Na_2SO_4, and $SrCl_2 \cdot 6H_2O$) were purchased from Sigma-Aldrich (Steinheim, Germany).

With respect to the solvents used in the extraction: methanol (LiChrosolv®) was supplied by Merck (Darmstadt, Germany); dichloromethane, toluene and ethyl acetate ("for organic residue analysis" grade) were purchased from J.T.Baker (Deventer, The Netherlands); and 1,2-dichlorobenzene (anhydrous, 99 %) and 1-butyl-3-methylimidazolium hexafluorophosphate ([BMIM][PF_6], ≥97.0 %) were purchased from Sigma-Aldrich (Steinheim, Germany). Concerning solvents for chromatography: methanol, ultrapure water (UPW) and acetonitrile (Optima® LC/MS grade) were purchased from Fischer Chemical (Loughborough, UK), while toluene (Chromasolv®) and *n*-hexane (SupraSolv®) were purchased from Merck (Darmstadt, Germany).

2.2. Preparation of the fullerene suspensions 1.0 ± 0.05 mg of C_{60} fullerene powder was weighed in tared quartz vials. 20.0 ± 0.02 ml of the corresponding water medium were pipetted inside each vial, obtaining a suspension with a concentration 50 ± 2.5 mg l^{-1} (~69 ± 3.5 µM). Vials were loosely capped with previously slitted aluminium foil, allowing free ambient air exchange while preventing potential contamination from dust deposition.

Nine different media were prepared, simulating different environmental scenarios (see **Table 1**). Suspensions 1, 2 and 3 allowed the study of the effects of salinity; suspensions 1, 4 and 5 allowed the study of the effects of pH; and suspensions 1, 6 and 7 allowed the study of the effects of humic substances content. These three parameters are known to control the colloidal chemistry of nC_{60} [32, 51, 52] and, subsequently, the number of C_{60} molecules located in the surface of the aggregates. In addition, experiment 8, reproducing artificial freshwater (AFW), and experiment 9, artificial seawater (ASW), were also

conducted. The salinity, the pH and the concentration of humic acids were studied because they have been shown to regulate the size of nC_{60} aggregates [32, 51, 52], which can be a relevant factor if we assume that functionalization of fullerenes is a surface reaction.

Media with a high ionic strength (46,000 µS cm^{-1}, suspensions 3 and 9) were prepared in order to simulate the salinity of seawater [53] by dissolving NaCl (23.93 g l^{-1}), $MgCl_2 \cdot 6H_2O$ (10.80 g l^{-1}), Na_2SO_4 (4.01 g l^{-1}), $CaCl_2 \cdot 2H_2O$ (1.50 g l^{-1}), KCl (0.677 g l^{-1}), $NaHCO_3$ (196.0 mg l^{-1}), KBr (98.0 mg l^{-1}), H_3BO_3 (26.0 mg l^{-1}), $SrCl_2 \cdot 6H_2O$ (24.0 mg l^{-1}), and NaF (3.0 mg l^{-1}) in UPW. Media with an intermediate ionic strength (970 µS/cm, suspensions 2 and 8) were prepared according to Lipschitz and Michel (2002) [54] by dissolving NaCl (175.3 mg l^{-1}), $CaCl_2$ (22.2 mg l^{-1}), $MgCl_2$ (19.0 mg l^{-1}) and KCl (14.9 mg l^{-1}) in UPW. The remaining suspensions were prepared with UPW (5.8 µS/cm), adjusting the humic acid contents and the pH with NaOH(aq) and HCl(aq) when necessary.

2.3. Weathering, sampling and extraction Two series of experiments were performed: one with sunlight irradiation and another in dark conditions. Quartz vials for irradiated experiments were gently vortexed during 1.0 min and placed in a SunTest apparatus from Heraeus (Hanau, Germany), equipped with a Xenon arc lamp that provided an irradiance of 600 W m^{-2} ($Ee_{\lambda=365\ nm}$ = 3.180 mW cm^{-2} and $Ee_{\lambda=312\ nm}$ = 2.283 mW cm^{-2}). Quartz vials for non-irradiated experiments were covered with aluminium foil, placed in a 10-position magnetic stirrer and agitated with PTFE-coated magnetic bars.

Aliquots were taken from each vial periodically until the experiments were finalized, after 48 and 96 hours for the irradiated and the non-irradiated series, respectively. The optimization of the extraction method is described in the Supplementary Information **(Text S1**). Briefly, 500 µL of sample were placed in a 3 ml glass vial containing 1.00 ml of toluene spiked with ^{13}C-enriched C_{60} fullerene at a concentration of 10 ng mL^{-1}. The vial was capped and vortexed during 1 min. After separation of phases, an aliquot of ~1 ml of toluene extract was transferred with a Pasteur pipette into a 1.5 ml amber LC vial for its instrumental analysis

2.4. Instrumental analysis The HPLC-HRMS method was based on a previously published one [21]. Some modifications were introduced in order to optimize the separation and detection of C_{60} transformation products.

The optimization of the HPLC-HRMS method is described in the Supplementary Information **(Texts S2 and S3)**. HPLC separation was achieved by non-aqueous LC, using an Acquity UPLC System (Waters, Milford, MA, USA) equipped with a COSMOSIL™ Buckyprep column (150 × 2.0 mm; particle size, 5 µm; pore size, ~120 Å) from Nacalai Tesque Inc. (Kyoto, Japan). The mobile phase consisted of an isocratic flow of toluene and methanol, at a 9 to 1 ratio, flowing at 0.4 $ml.min^{-1}$ during 20 min. 20 µl of extract was injected in each run.

The system was coupled to a Q Exactive™ mass spectrometer (Thermo Fischer Scientific, San Jose, CA, USA) with a hybrid atmospheric pressure chemical ionisation / atmospheric pressure photoionisation (APCI/APPI) source Ion Max (Thermo Fischer Scientific, San Jose, CA, USA) working in APPI mode. Ionisation was carried out in negative polarity and source parameters were set as follows: sheath gas, 40 a.u.; auxiliary gas, 25 a.u.; spare gas, 1 a.u.; spray voltage, 5.0 kV; capillary and probe heater temperatures, 300 °C and 400 °C, respectively; and S-lens RF, 90 %. Acquisition was performed in full scan from m/z = 300 to 1,600 with a resolution of 140,000 full width at half maximum (FWHM).

2.5. Precautions and safety considerations Precautions and safety considerations are summarised in the **Text S4** of the Supplementary Information.

3. Results and discussion

3.1. Identification of transformation products Up to ten transformation products of C_{60} fullerene were detected (see **Table 2**). All the experimental m/z signals could be tentatively assigned to empirical formulae with mass accuracies <1.5 ppm (<0.5 ppm, in those molecules smaller than 1,000 Da). The identified compounds also presented the isotopic patterns of C_{60} (with a predominant $[^{12}C_{60}]^{\cdot -}$ signal, followed by the signals $[^{12}C_{59}\ ^{13}C]^{\cdot -}$ and $[^{12}C_{58}\ ^{13}C_2]^{\cdot -}$, with relative intensities of ~0.65 and ~0.22, respectively) or C_{120} (with a predominant $[^{12}C_{119}\ ^{13}C]^{\cdot -}$ signal, and the signals $[^{12}C_{120}]^{\cdot -}$ and $[^{12}C_{118}\ ^{13}C_2]^{\cdot -}$ with relative intensities of ~0.77 and ~0.64).

The tentatively identified compounds included several oxidized fullerenes, one mono-oxidized dimer of C_{60} fullerene and three signals corresponding to dioxidized dimers of C_{60} fullerenes. Standards of these compounds were not commercially available.

A single peak of mono-oxidised fullerene was observed with a retention time of 3.50 min (see **Figure 1b)**. The structural isomers that can be assigned to the formula $C_{60}O$ are the C_{60} epoxide (abbreviated [6,6]$C_{60}O$) and the C_{60} oxido-annulene (abbreviated [5,6]$C_{60}O$) [55], both represented in the **Figure S5** of the Supporting Information. Both molecules can be generated by oxidation, under harsh oxidative conditions, i.e. with dimethyldioxirane [56], or by reaction with ozone, as reported before [57]. While the thermolysis of the ozonide intermediate produces [6,6]$C_{60}O$, its photolytic scission produces [5,6]$C_{60}O$. Therefore, [6,6]$C_{60}O$ is likely to be predominant in dark experiments, while [5,6]$C_{60}O$ would be formed by irradiation but the simultaneous generation of both products cannot be excluded.

The other two peaks in **Figure 1.b**, with retention times (t_R) of ~2 and 3.07 min corresponded to a matrix interference and to an APPI-adduct of the C_{60} peak, respectively.

Three $C_{60}O_2$ signals were observed: one peak at t_R=3.73 (*k'*=3.0), another at t_R=6.92 (*k'*=6.2) and a third signal at t_R=8.71. While the third peak is believed to be a chromatographic artefact (attributed to the in-source fragmentation of $C_{60}O_3$) the first two peaks can be assigned to transformation products, either C_{60} dicarbonyl and to diepoxidized C_{60}. The C_{60} dicarbonyl is generated by decomposition of the C_{60} dioxetane, a highly unstable intermediate produced by the addition of a $^1O_2$ to a C_{60}'s [6,6] bond [45]. Nevertheless, the C_{60} dicarbonyl is unlikely to be generated in the present experiments since its precursor, the C_{60} dioxetane, is only generated under harsh irradiation conditions. The presence of epoxy groups instead of carbonyl groups on mono-, di- and tri-oxidised fullerenes was also confirmed by FTIR and ^{13}C NMR after light exposure in solution [58]. More likely, the two peaks belong to any of the eight regioisomers of diepoxidized C_{60} fullerene that can exist [59] (see **Figure 2**). In previous works two chromatographic peaks have been also reported corresponding to diepoxides of C_{60} fullerene, after reaction with *m*-chloroperoxybenzoic acid [59, 60] or with ozone [61]. While the predominant peak has been previously identified as the isomer *cis1*, which is also the most stable diepoxide according to computational calculations [60, 62], the less intense peak has been assigned to an unresolved mixture of diepoxidized fullerenes [59], to the equatorial isomer [60], and to the isomer *cis2* [61]. Therefore, the peak at *k'*=3.0, which was the predominant one in all the experiments, was assigned to the *cis1* regioisomer, while the peak at *k'*=6.2 may be either the *cis2* or the *equatorial* isomer. To further characterize both diepoxides, the toluene extract was fractionated and the fractions

corresponding to the first and second peaks were analysed by infrared (IR) spectroscopy. However, due to the low concentrations and to the interference from column bleed, non-conclusive results were obtained.

As can be seen in **Figure 1d**, four signals were detected with the m/z of trioxidized C_{60} fullerenes. The signals at t_R=3.73 and t_R=6.92 min are APPI-adducts of $C_{60}O_2$ isomers, which have already been described. In contrast, the other two signals belong to new transformation products (*k'*=3.8 and *k'*=6.4, the second one being the most intense). The presence of the ozonide $C_{60}O_3$ was discarded because of its instability [63]. Instead, according to previous theoretical and experimental works [60, 62, 64], the presence of different isomers of the triepoxidized C_{60} fullerene was considered. Among the 43 possible regioisomers of triepoxidized C_{60} fullerene, the most abundant was the one that contains the three oxygen atoms in the [6,6] bonds of the same benzene ring (C_{3v} symmetry, see **Figure S6a**), which is thermodynamically favoured [65]. The least abundant detected compounds were likely to present the three epoxide groups in adjacent [6,6] bonds (see **Figures S6b** and **S6c**): two groups in the same benzene ring and the third group in the most nearby [6,6] bond of an adjacent benzene ring.

Similarly, a single tetraoxidized transformation product was detected (see **Figure S7**). To our knowledge, the stability and relative predominance of the C_{60} tetraepoxide regioisomers has not been addressed to date in any previous work. According to the stability criteria that have been employed for the triepoxides discussion, the most stable regioisomer of the tetraepoxides family should be the one with three functional groups in the same benzene ring and the fourth epoxide group in an adjacent [6,6] bond. Epoxides with formula $C_{60}O_5$ or $C_{60}O_6$ have been observed elsewhere after 1-3 minutes of ozonolysis [66], but were short-lived. IR evidence of cage rupture was found for high degree of oxygenation [67]. The softer oxidation conditions employed in our work could also account for their nondetection.

The formation of four fullerene dimers was also observed (**Figure 3**), corresponding to a compound with formula $(C_{60})_2O$ and three compounds with formula $(C_{60})_2O_2$. The signal of $(C_{60})_2O$ (*k'*=7.2) was already elucidated [68] (see chromatogram and proposed structure in **Figure 4**). This compound is generated by [2+2] reaction of [6,6]$C_{60}O$ with the [6,6] bond of a C_{60} fullerene, originating a molecule with two C_{60} units linked by a furane-like ring.

Regarding $(C_{60})_2O_2$, three different chromatographic peaks were observed (I, II and III in **Figure 3**). The peak I (*k'*=8.2) appeared as a well-resolved chromatographic peak while the peaks II (*k'*=15.5) and III (*k'*=19.2) corresponded to mixtures of chromatographically unresolved isomers. Two different types of structures could be assigned to these three peaks: an epoxidized $(C_{60})_2O$, which may be produced either by the [2+2] reaction of two [6,6]$C_{60}O$ molecules or by epoxidation of a $(C_{60})_2O$ molecule; or a bis-linked compound, consisting in two C_{60} units fused via two adjacent furane-like rings. The furane-like rings links may be separated by [6,6] bonds or by [5,6] bonds, as described elsewhere [69]. In this case, the assignment of a structure to each peak was less clear. On the basis of the retention of each peak and the polarity of the compounds, peak I may be the bis-linked compound, while peaks II and III were most likely related to a mixture of regioisomers, as described in **Figure 3**.

In a previous work, $(C_{60})_2O$ and $(C_{60})_2O_2$ have been identified as degradation products of C_{60} fullerene in solid state [70]. Also, the presence of dimerized fullerenes were suspected after UV-spectroscopy analyses in aerosol samples degraded with ozone [69]. However, according to our knowledge, this is the first time that fullerene dimers are unambiguously proven to be a component of nC_{60} produced under environmentally relevant conditions. Neither $(C_{60})_2$ nor any molecule containing more than two sub-units of C_{60} fullerene were detected in the present work.

Finally, hydroxylated fullerenes, or fullerenols, were not detected in any degradation experiment, including the analysis of the toluene extracts, the analysis of extracts by other organic solvents (see **Text S1**) and the analysis of water suspensions by direct injection inside the mass spectrometer. The use of an electrospray source, which has been used elsewhere for analysing these compounds [71], was also fruitless. In the literature, fullerenols were recently reported in soils incubated under ultraviolet irradiation [50] and in water suspensions prepared by direct sonication without light exposure [72, 73]. Therefore, in a complementary experiment, a C_{60} suspension was prepared in ultrapure water at pH 12 and was sonicated in an ultrasonic bath for 1 hour. After extraction with toluene, the analysis of the extract revealed a series of prominent peaks with molecular ions $[C_{60}O_xH_{(x-1)}]\cdot^-$ (x=1-6), presumably belonging to deprotonated fullerenols. The intensities of these signals were ~10^4 times lower than that of the precursor, C_{60} fullerene, and, as can be seen in **Figure S8,** all the fullerenols eluted at a lower retention time than C_{60} (selectivity $\alpha \leq 0.55$), in contrast to the other compounds listed in **Table 2**. It can be

concluded that fullerenols are not produced in water suspension in normal environmental conditions, as it was not observed previously in ultrapure water [48].

3.2. Kinetics of degradation of C_{60} fullerene in ultrapure water Table 3 summarizes the results obtained when plotting the concentration of fullerene epoxides against the time of experiment. The concentrations of the degradation products were normalized by the concentration of precursor C_{60}, as justified in the **Supplementary Text S5** and **Figure S9**

The presence or absence of sunlight affected decisively the generation of epoxides. Higher concentrations of transformation products were observed in experiments with sunlight in comparison to experiments in the dark. E.g., concentrations of $C_{60}O_4$, $C_{60}O_3$ (*k'*=3.8) and $C_{60}O_3$ (*k'*=6.4) were 19±11, 7.3±5.5 and 2.9±1.3 times higher in the presence of sunlight than in the dark.

In irradiated experiments, during the initial hours, the concentration of epoxides increased rapidly and more or less linearly; then, it reached a maximum concentration, which in experiments performed in ultrapure water was observed at ~1.5 h); and, during the following 46.5 hours the concentration of epoxides stabilized or decreased (see **Figures S10** and **S11**)..

In contrast, in experiments without simulated sunlight irradiation, the concentration of epoxides increased steadily and linearly during the 96 hours of the experiment. This general behaviour was observed for all the detected epoxides except for $C_{60}O_3$ (*k'*=3.8), which reached a peak concentration after only 24 hours of agitation and stabilized.

As can be seen in **Table 3**, the generation of epoxides was much slower in the dark (the slopes of the linear regressions are two orders of magnitude lower than in the irradiated experiment). Therefore, the epoxidation of fullerenes was catalysed by light, but light exposure itself was responsible for the disappearance of these compounds after 72 hours. This suggests that the stability of fullerene epoxides is limited, but the identity of the next generation of transformation products remains unknown. The generation of higher epoxides, or even open-cage transformation products, can be hypothesized.

With regards to dimers with one and two furane-like rings, their generation in ultrapure water experiments, with and without sunlight irradiation, can be seen in **Figure S10**. As can be seen (**Figure S10.a**), $C_{120}O$ was not found in experiments without light irradiation. It's generation may be too slow to be observed under these conditions. When simulated

sunlight was applied, $C_{120}O$ was detected after 6 hours and its concentration increased linearly (in ultrapure water, r=0.95, p=0.013) with an apparent constant of 2.62×10^{-7} h^{-1}. This slope was the flattest of all the compounds, 20 times smaller than that of $C_{60}O_3$ (*k'*=3.8), which was the least abundant epoxide detected. $C_{120}O$ was not only the least abundant degradation product of C_{60} but it also was the only one that increased monotonically through time. This could potentially become a useful tool for dating the presence of C_{60} fullerene in the environment.

Finally, $C_{120}O_2$ (*k'*=8.2) was detected in both types of experiments, when suspended in the dark and with light exposure, but a different behaviour was observed in each case. The dimer was generated by solvation and, in the dark, its concentration remained stable during the first 48 hours, after which it increased significantly (see **Figure S10.b**). In contrast, when irradiated, the concentration of $C_{120}O_2$ decreased significantly (see **Figure S10.d**), indicating the lability of this compound.

3.3. Role of salinity, humic acids and pH As detailed in **Table 1**, degradation experiments were performed at three conductivities (5.8, 970 and 46,000 µS cm^{-1}), at three pHs (6.00, 7.00 and 8.15), and with varying concentrations of humic acids (0, 0.3 and 2.25 mg l^{-1}). Overall, drastic differences were not observed when modifying these parameters, since the profile of transformation products and their general behaviour remained unchanged, and these physicochemical properties just modulated the results obtained.

Regarding salinity, in experiments without light exposure, higher ionic strengths resulted in higher concentrations of epoxides and dimers (**Figure S11**). This trend cannot be satisfactorily explained by the DLVO theory. According to this model, an increase in the salinity of the medium leads to the suppression of the electric double barrier of the aggregates, which favours the dominance of the attractive van der Waals forces among nC_{60}. In this scenario, larger aggregates are stabilized, with smaller surface-to-volume ratio. Assuming that functionalization is a surface reaction, larger aggregates would generate less TPs. However, the opposite was observed in the present work. Our hypothesis is that a higher ionic strength leads to a less negative ζ-potential [74]. In this scenario, the water molecules surrounding the aggregates would be oriented in a more flexible manner, enhancing the diffusion potential of the reactive species as dissolved ozone and $^1O_2$.

In contrast to all this, irradiated experiments were not affected by changes in the medium salinity.

Regarding pH, in experiments without irradiation it was inversely related to the concentration of transformation products. Slightly lower concentrations of transformation products were identified at pH=8.15 than at pH=6.00 (**Figure S12**). Again, irradiated experiments were not significantly affected by changes of the pH.

Finally, the presence of humic acids, which are known to modulate the size and shape of nC_{60} aggregates [38, 75], had an impact on the formation of TPs when irradiated by simulated sunlight: The concentration of epoxides increased with higher concentrations of humic acids and decreased after 24 h of irradiation, while the concentrations of dimers were barely affected (**Figure S13**). This can be attributed to the fact that humic substances, when irradiated with ultraviolet light (especially from UV-A and UV-B regions) can produce reactive oxygen species (ROS) such as $^1O_2$, O_2, or H_2O_2 [76]. Irradiated humic acids generate radicals that enhance the epoxidation of fullerenes, as observed in the present work. In absence of light, the concentration of humic acids did not present any effect in the generation of TPs.

3.4. Environmental implications The presence of salts and organic matter in natural waters favours the presence of fullerene transformation products (epoxides and dimers). This was corroborated in the experiments performed in AFW (suspension 8: 970 µS/cm, pH=7.00±0.01 and [HA]=2.25 mg l^{-1}) and ASW (suspension 9: 46,000 µS/cm, pH=8.15±0.01 and [HA]=0.3 mg l^{-1}), as can be seen in **Figure 4**.

The presence of fullerene epoxides and dimers in the real environment is of relevance, given the different properties and behaviour of these transformation products. It is known that functionalised carbon nanotubes and fullerenes adsorb pollutants onto their surfaces with stronger binding than bare nanotubes [77, 78]. Therefore, the potential of fullerenes of immobilizing and transporting other co-contaminants in the aquatic environment is likely to increase progressively after their disposal and weathering [79, 80]. This may affect the ecosystem indirectly, by changing the bioavailability of these other co-contaminants, and also directly, because of the different toxicity of fullerenes and fullerene epoxides. In this regard, recent studies have found relevant differences in soil microbial communities when exposed to unaltered nC_{60} and photodegraded nC_{60} [81]. Also, the presence of functional groups on the surface of the aggregates may enhance

their stability in water. This would have implications in the transport potential and water-sediment partition coefficients of fullerenes, as studied elsewhere [21].

It is also important to study toxicity, behaviour and sorption capabilities of fullerene dimers to fully understand the implications of their photo-transformation in the real environment.

However, in the environment the occurrence of transformation products may be limited, since C_{60} fullerene seems to be comparatively stable (see the relative abundances of epoxides in **Table 2**). Moreover, sunlight showed an ambivalent effect on the generation of epoxides: whilst it accelerated their generation at first, it also enhanced their elimination after ~24 hours. Therefore the persistence of these transformation products in the environment is likely to be limited. This excludes surface waters located in shady areas, deeper waters, groundwater and closed wells, where the epoxidation of fullerenes would be lower and increase linearly as suggested in our simulations without light exposure.

With respect to the persistence of these compounds, it may also be important to consider the role of hetero-aggregation, i.e. their persistence/degradability in presence of inorganic particulate material. Particulate matter/turbidity in a water column may scatter incident light, greatly reducing penetration of light beneath the surface [82]. Therefore, fullerene epoxides may be photodegraded more slowly when they are attached to particles than when they are freely suspended as fullerene homo-aggregates.

Moreover, the concentrations of fullerene C_{60} transformation products may be significantly higher close to the disposal point of wastewater treatment plants, where they may act as pseudo-persistent pollutants. This point was confirmed in a real sample from the Besòs River (close to Barcelona) taken near a wastewater disposal point. 35 l of surface water were spiked with $^{13}C_{60}$ and extracted by LLE with toluene in a 10:1 ratio. The extract was concentrated to 1.0 ml by rotatory evaporation and injected. $C_{60}O$ was detected and determined semi-quantitatively, resulting in an approximate concentration of ~2 ng l^{-1} (see chromatogram in **Figure S14**). The environmental effects of fullerene transformation products, if confirmed, may be more pronounced on a local-scale in hotspots like this.

Acknowledgements

This work was supported by the Spanish Ministry of Economy and Competitiveness, through the project NANO-transfer (ERA-NET SIINN PCIN-2015-182-CO2-01); by the UK Natural Environment Research Council, through the project "Trojan horses" (NE/L006782/1); and by the Generalitat de Catalunya (Consolidated Research Groups "2014 SGR 418 – Water and Soil Quality Unit" and "2014 SGR 291 – ICRA"). The authors would like to acknowledge the helpful assistance of Dr. Chaler and Mrs. Fanjul from the mass spectrometry services of IDAEA-CSIC.

Conflict of interest

The authors state that there are not actual or potential conflicts of interest.

442 **Table 1.** Experimental design showing the salinity, pH and humic acid concentration
443 (c_{HA}) of the aqueous dispersant media.

#	Description	Conductivity (µS/cm)	pH	c_{HA} (mg l^{-1})
Experiment 1	Reference pure water	**5.8**	**7 ± 0.1**	**0**
Experiment 2	Intermediate salinity	**970**	7.00 ± 0.01	0
Experiment 3	High salinity	**46,000**	7.00 ± 0.01	0
Experiment 4	Acidic pH	<200	**6.00 ± 0.01**	0
Experiment 5	Basic pH	<200	**8.15 ± 0.01**	0
Experiment 6	High c_{HA}	5.8	7 ± 0.1	**2.25**
Experiment 7	Intermediate c_{HA}	5.8	7 ± 0.1	**0.3**
Experiment 8	Artificial freshwater	**970**	**7.00 ± 0.01**	**2.25**
Experiment 9	Artificial seawater	**46,000**	**8.15 ± 0.01**	**0.3**

444

Table 2. Summary of transformation products and their tentatively proposed structures.

#	*k'*	Relative intensity*	Proposed compound	Proposed formula	Molar mass (g mol^{-1})	Exp. m/z*	Exp. abundance*	Proposed ion	Theoretical m/z	Theoretical abundance	m/z error (ppm)
1	2.6	6.4×10^{-5}	C_{60} epoxide ([6,6]C_{60}O)	$C_{60}O$	736.6	735.9953	100	$[^{12}C_{60}\,O]^{\cdot-}$	735.9955	100	0.27
						736.9988	72	$[^{12}C_{59}\,^{13}C_1\,O]^{\cdot-}$	736.9988	65	0.00
2	3.0	6.6×10^{-5}	Diepoxidized C_{60} (*cis-1* isomer)	$C_{60}O_2$	752.6	751.9905	100	$[^{12}C_{60}\,O_2]^{\cdot-}$	751.9904	100	0.13
						752.9940	68	$[^{12}C_{59}\,^{13}C_1\,O_2]^{\cdot-}$	752.9937	65	0.40
3	6.2	3.3×10^{-5}	Diepoxidized C_{60}	$C_{60}O_2$	752.6	751.9905	100	$[^{12}C_{60}\,O_2]^{\cdot-}$	751.9904	100	0.13
						752.9941	68	$[^{12}C_{59}\,^{13}C_1\,O_2]^{\cdot-}$	752.9937	65	0.53
4	3.8	$<1.0\times10^{-7}$	Triepoxidized C_{60}	$C_{60}O_3$	768.6	767.9856	100	$[^{12}C_{60}\,O_3]^{\cdot-}$	767.9853	100	0.39
						768.9883	69	$[^{12}C_{59}\,^{13}C_1\,O_3]^{\cdot-}$	768.9886	65	0.39
5	6.4	5.5×10^{-5}	Triepoxidized C_{60} (C_{3v} sym.)	$C_{60}O_3$	768.6	767.9850	100	$[^{12}C_{60}\,O_3]^{\cdot-}$	767.9853	100	0.39
						768.9884	67	$[^{12}C_{59}\,^{13}C_1\,O_3]^{\cdot-}$	768.9886	65	0.26
6	10.5	1.4×10^{-4}	Tetraepoxidized C_{60}	$C_{60}O_4$	784.6	783.9800	100	$[^{12}C_{60}\,O_4]^{\cdot-}$	783.9802	100	0.26
						784.9834	68	$[^{12}C_{59}\,^{13}C_1\,O_4]^{\cdot-}$	784.9836	65	0.25
7	7.2	1.3×10^{-5}	C_{60} dimer linked by 1 furane-like ring	$(C_{60})_2O$	1457	1455.9958	76	$[^{12}C_{120}\,O]^{\cdot-}$	1455.9955	77	0.21
						1456.9992	100	$[^{12}C_{119}\,^{13}C_1\,O]^{\cdot-}$	1456.9988	100	0.27
8	8.2	2.7×10^{-5}	C_{60} dimer linked by 2 furane-like rings	$(C_{60})_2O_2$	1473	1471.9888	75	$[^{12}C_{120}\,O_2]^{\cdot-}$	1471.9904	77	1.09
						1472.9924	100	$[^{12}C_{119}\,^{13}C_1\,O_2]^{\cdot-}$	1472.9937	100	0.88
9	15.5	9.8×10^{-6}	Mixture of other unresolved dimers	$(C_{60})_2O_2$	1473	1471.9890	72	$[^{12}C_{120}\,O_2]^{\cdot-}$	1471.9904	77	0.95
						1472.9933	100	$[^{12}C_{119}\,^{13}C_1\,O_2]^{\cdot-}$	1472.9937	100	0.27
10	19.2	9.9×10^{-5}	Mixture of other unresolved dimers	$(C_{60})_2O_2$	1473	1471.9888	78	$[^{12}C_{120}\,O_2]^{\cdot-}$	1471.9904	77	1.09
						1472.9922	100	$[^{12}C_{119}\,^{13}C_1\,O_2]^{\cdot-}$	1472.9937	100	1.02

* Defined as the ratio between the areas of each transformation product peak and that of C_{60} fullerene after 48 h of agitation in ultrapure water with irradiation.

** Isotopic pattern, defined as the average intensity of all the spectra acquired in the chromatographic peak with an intensity >10 % of the maximum height.

Table 3. Behaviour of the fullerene epoxides in experiments suspended in ultrapure water.

Compound		Experiment with light exposure		Experiment without light exposure	
Formula	***k'***	**Linear range[1]**	**Slope[2] (h^{-1})**	**Linear range[1]**	**Slope[2] (h^{-1})**
$C_{60}O$	2.6	0 h to 1.0 h (r=0.90)	2.6×10^{-5}	0 h to 96 h (r=0.93)	7.3×10^{-7}
$C_{60}O_2$	3.0	0 h to 1.5 h (r=0.94)	1.4×10^{-4}	0 h to 96 h (r=0.91)	9.6×10^{-7}
$C_{60}O_2$	6.2	0 h to 1.5 h (r=0.98)	9.0×10^{-5}	0 h to 96 h (r=0.91)	1.0×10^{-6}
$C_{60}O_3$	3.8	0 h to 1.5 h (r=0.98)	5.6×10^{-6}	0 h to 24 h (r=0.91)	8.2×10^{-8}
$C_{60}O_3$	6.4	0 h to 1.5 h (r=0.98)	4.2×10^{-5}	0 h to 96 h (r=0.97)	7.5×10^{-7}
$C_{60}O_4$	10.5	0 h to 1.5 h (r=1.00)	1.0×10^{-4}	0 h to 96 h (r=0.94)	2.5×10^{-7}

[1]Defined as the interval of time in which the normalized concentration of epoxide evolved linearly, this is, with a Pearson Index >0.90.
[2]Calculated for comparison purposes as the slope of the linear regression obtained when representing the concentration of epoxide, normalized by the concentration of C_{60}, against the time of exposure.

Figure 1. Extracted Ion Chromatograms of m/z=720.0005±0.0010 (*a*), 735.9954±0.0010 (*b*), m/z=751.9905±0.0010 (*c*), m/z=767.9856±0.0010 (*d*) and 783.9800±0.0010 (*e*).

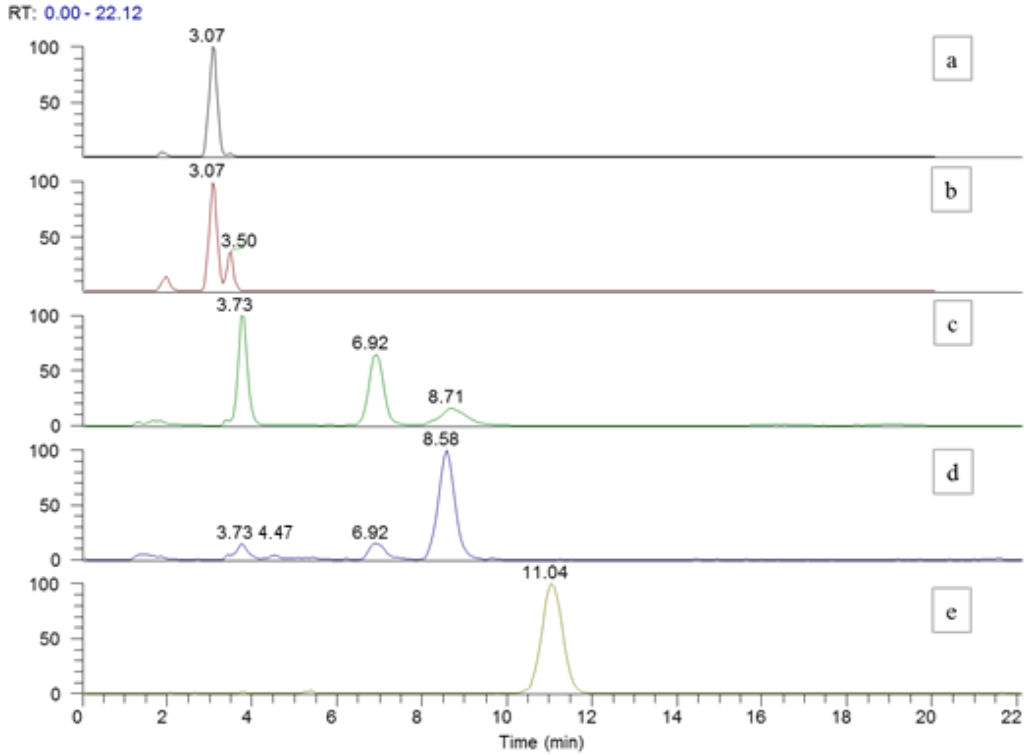

Figure 2. Relative positions of the epoxide functional groups in the eight isomers of diepoxidized fullerene C_{60}. All the regioisomers are produced by the addition of oxygen atoms in [6,6] bonds.

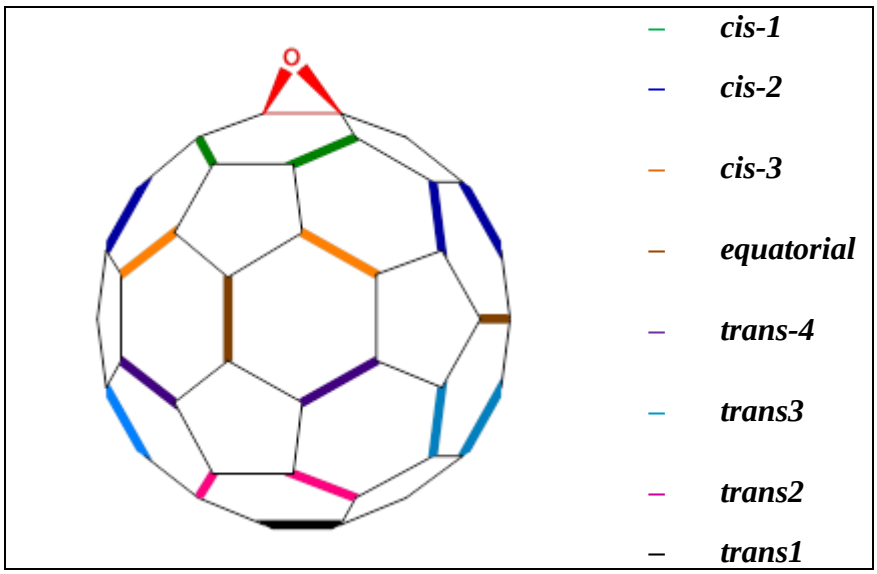

Figure 3. Extracted Ion Chromatogram of m/z=1455.9958 (top) and m/z=1471.9888 (bottom), corresponding to oxidized and dioxidized fullerene dimers, and their proposed structures.

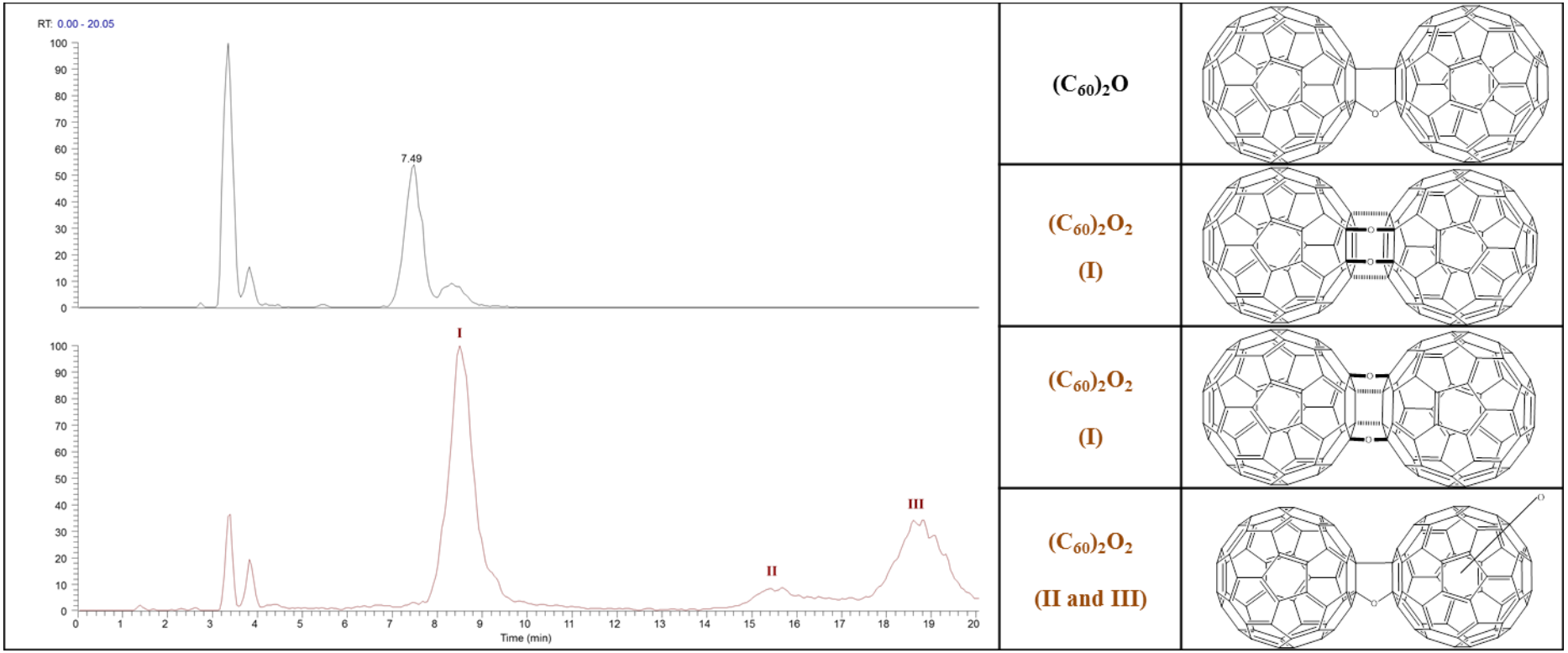

Figure 4. Occurrence of degradation products of C_{60} fullerene after 48 hours of simulated sunlight irradiation in ultrapure water (black bars), in artificial freshwater (grey bars) and in artificial seawater (dashed bars). The concentrations of degradation products were estimated semi-quantitatively, because of the absence of commercially available analytical standards, considering that they had the same response factor than C_{60} fullerene.

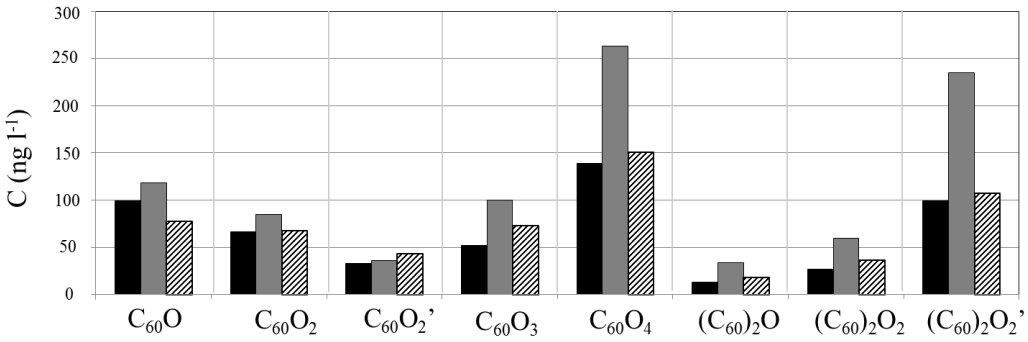

References

[1] H.W. Kroto, J.R. Heath, S.C. O'Brien, R.F. Curl, R.E. Smalley, C 60: buckminsterfullerene, Nature 318(6042) (1985) 162-163.

[2] S. Vidal, Glycofullerenes: Sweet fullerenes vanquish viruses, Nat Chem 8(1) (2016) 4-6.

[3] R. Bakry, R.M. Vallant, M. Najam-ul-Haq, M. Rainer, Z. Szabo, C.W. Huck, G.K. Bonn, Medicinal applications of fullerenes, International journal of nanomedicine 2(4) (2007) 639.

[4] K. Jinno, K. Yamamoto, J.C. Fetzer, W.R. Biggs, C60 as a stationary phase for microcolumn liquid chromatographic separation of polycyclic aromatic hydrocarbons, Journal of Microcolumn Separations 4(3) (1992) 187-190.

[5] R.N. Goyal, V.K. Gupta, N. Bachheti, R.A. Sharma, Electrochemical sensor for the determination of dopamine in presence of high concentration of ascorbic acid using a Fullerene-C60 coated gold electrode, Electroanalysis 20(7) (2008) 757-764.

[6] H. Park, J. Park, A.K.L. Lim, E.H. Anderson, A.P. Alivisatos, P.L. McEuen, Nanomechanical oscillations in a single-C60 transistor, Nature 407(6800) (2000) 57-60.

[7] R. Haddon, A. Perel, R. Morris, T. Palstra, A. Hebard, R. Fleming, C60 thin film transistors, Applied Physics Letters 67(1) (1995) 121-123.

[8] C.J. Brabec, S. Gowrisanker, J.J.M. Halls, D. Laird, S. Jia, S.P. Williams, Polymer–Fullerene Bulk-Heterojunction Solar Cells, Advanced Materials 22(34) (2010) 3839-3856.

[9] B.C. Thompson, J.M.J. Fréchet, Polymer-fullerene composite solar cells, Angewandte Chemie International Edition 47(1) (2008) 58-77.

[10] L.T. Lukich, T.E. Duncan, C.M. Lansinger, Use of fullerene carbon in curable rubber compounds, Google Patents, 1998.

[11] B. Jurkowska, B. Jurkowski, P. Kamrowski, S. Pesetskii, V. Koval, L. Pinchuk, Y.A. Olkhov, Properties of fullerene-containing natural rubber, Journal of applied polymer science 100(1) (2006) 390-398.

[12] T.K. Daly, P.R. Buseck, P. Williams, C.F. Lewis, Fullerenes from a Fulgurite, Science 259(5101) (1993) 1599-1601.

[13] L. Becker, J.L. Bada, Fullerenes in Allende meteorite, Nature 372 (1994) 507.

[14] L. Becker, T.E. Bunch, L.J. Allamandola, Higher fullerenes in the Allende meteorite, Nature 400(6741) (1999) 227-228.

[15] D. Heymann, A. Korochantsev, M.A. Nazarov, J. Smit, Search for fullerenes C60 and C70 in Cretaceous–Tertiary boundary sediments from Turkmenistan, Kazakhstan, Georgia, Austria, and Denmark, Cretaceous Research 17(3) (1996) 367-380.

[16] L.I. Yanfang, L. Handong, Y.I.N. Hongfu, S.U.N. Jing, C.A.I. Hou'an, R.A.O. Zhu, R.A.N. Fanlin, Determination of Fullerenes (C60/C70) from the Permian-Triassic Boundary in the Meishan Section of South China, Acta Geologica Sinica - English Edition 79(1) (2005) 11-15.

[17] Z. Su, W. Zhou, Y. Zhang, New insight into the soot nanoparticles in a candle flame, Chemical Communications 47(16) (2011) 4700-4702.

[18] A.J. Tiwari, M. Ashraf-Khorassani, L.C. Marr, C60 fullerenes from combustion of common fuels, Science of the Total Environment 547 (2016) 254-260.

[19] E. Emke, J. Sanchis, M. Farre, P. Bäuerlein, P. de Voogt, Determination of several fullerenes in sewage water by LC HR-MS using atmospheric pressure photoionisation, Environmental Science: Nano 2(2) (2015) 167-176.

[20] J. Sanchís, N. Berrojalbiz, G. Caballero, J. Dachs, M. Farré, D. Barceló, Occurrence of Aerosol-Bound Fullerenes in the Mediterranean Sea Atmosphere, Environmental Science & Technology 46(3) (2012) 1335-1343.

[21] J. Sanchís, C. Bosch-Orea, M. Farré, D. Barceló, Nanoparticle tracking analysis characterisation and parts-per-quadrillion determination of fullerenes in river samples from Barcelona catchment area, Analytical and bioanalytical chemistry 407(15) (2015) 4261-4275.
[22] J. Sanchís, D. Božović, N.A. Al-Harbi, L.F. Silva, M. Farré, D. Barceló, Quantitative trace analysis of fullerenes in river sediment from Spain and soils from Saudi Arabia, Analytical and bioanalytical chemistry 405(18) (2013) 5915-5923.
[23] A. Astefanei, O. Núñez, M.T. Galceran, Analysis of C_{60}-fullerene derivatives and pristine fullerenes in environmental samples by ultrahigh performance liquid chromatography-atmospheric pressure photoionization-mass spectrometry, Journal of Chromatography A 1365 (2014) 61-71.
[24] Ó. Núñez, H. Gallart-Ayala, C.P.B. Martins, E. Moyano, M.T. Galceran, Atmospheric Pressure Photoionization Mass Spectrometry of Fullerenes, Analytical Chemistry 84(12) (2012) 5316-5326.
[25] S. Utsunomiya, K.A. Jensen, G.J. Keeler, R.C. Ewing, Uraninite and Fullerene in Atmospheric Particulates, Environmental Science & Technology 36(23) (2002) 4943-4947.
[26] T. Laitinen, T. Petäjä, J. Backman, K. Hartonen, H. Junninen, J. Ruiz-Jiménez, D. Worsnop, M. Kulmala, M.-L. Riekkola, Carbon clusters in 50 nm urban air aerosol particles quantified by laser desorption-ionization aerosol mass spectrometer, International Journal of Mass Spectrometry 358(0) (2014) 17-24.
[27] J. Jehlička, O. Frank, V. Hamplová, Z. Pokorná, L. Juha, Z. Bohácek, Z. Weishauptová, Low extraction recovery of fullerene from carbonaceous geological materials spiked with C60, Carbon 43(9) (2005) 1909-1917.
[28] J. Sanchís, L.F.S. Oliveira, F.B. de Leão, M. Farré, D. Barceló, Liquid chromatography–atmospheric pressure photoionization–Orbitrap analysis of fullerene aggregates on surface soils and river sediments from Santa Catarina (Brazil), Science of the Total Environment 505 (2015) 172-179.
[29] A. Astefanei, O. Núñez, M.T. Galceran, Characterisation and determination of fullerenes: A critical review, Analytica chimica acta 882 (2015) 1-21.
[30] C.T. Jafvert, P.P. Kulkarni, Buckminsterfullerene's (C60) Octanol-Water Partition Coefficient (Kow) and Aqueous Solubility, Environmental Science & Technology 42(16) (2008) 5945-5950.
[31] M. Farré, S. Pérez, K. Gajda-Schrantz, V. Osorio, L. Kantiani, A. Ginebreda, D. Barceló, First determination of C 60 and C 70 fullerenes and N-methylfulleropyrrolidine C 60 on the suspended material of wastewater effluents by liquid chromatography hybrid quadrupole linear ion trap tandem mass spectrometry, Journal of Hydrology(Amsterdam) 383(1-2) (2010) 44-51.
[32] S. Deguchi, R.G. Alargova, K. Tsujii, Stable Dispersions of Fullerenes, C60 and C70, in Water. Preparation and Characterization, Langmuir 17(19) (2001) 6013-6017.
[33] G.V. Andrievsky, V.K. Klochkov, A.B. Bordyuh, G.I. Dovbeshko, Comparative analysis of two aqueous-colloidal solutions of C60 fullerene with help of FTIR reflectance and UV-Vis spectroscopy, Chemical Physics Letters 364(1-2) (2002) 8-17.
[34] B. Derjaguin, L. Landau, Theory of the stability of strongly charged lyophobic sols and of the adhesion of strongly charged particles in solutions of electrolytes, Acta physicochim. URSS 14(6) (1941) 633-662.
[35] K.L. Chen, M. Elimelech, Influence of humic acid on the aggregation kinetics of fullerene (C60) nanoparticles in monovalent and divalent electrolyte solutions, Journal of Colloid and Interface Science 309(1) (2007) 126-134.

[36] E.J.W. Verwey, J.T.G. Overbeek, J.T.G. Overbeek, Theory of the stability of lyophobic colloids, Courier Corporation1999.
[37] Q. Li, B. Xie, Y.S. Hwang, Y. Xu, Kinetics of C60 Fullerene Dispersion in Water Enhanced by Natural Organic Matter and Sunlight, Environmental Science & Technology 43(10) (2009) 3574-3579.
[38] C.W. Isaacson, D.C. Bouchard, Effects of Humic Acid and Sunlight on the Generation and Aggregation State of Aqu/C60 Nanoparticles, Environmental Science & Technology 44(23) (2010) 8971-8976.
[39] J.W. Arbogast, A.P. Darmanyan, C.S. Foote, F.N. Diederich, R. Whetten, Y. Rubin, M.M. Alvarez, S.J. Anz, Photophysical properties of sixty atom carbon molecule (C60), The Journal of Physical Chemistry 95(1) (1991) 11-12.
[40] J. Lee, J.D. Fortner, J.B. Hughes, J.-H. Kim, Photochemical Production of Reactive Oxygen Species by C60 in the Aqueous Phase During UV Irradiation, Environmental Science & Technology 41(7) (2007) 2529-2535.
[41] J. Lee, Y. Yamakoshi, J.B. Hughes, J.-H. Kim, Mechanism of C60 photoreactivity in water: Fate of triplet state and radical anion and production of reactive oxygen species, Environmental science & technology 42(9) (2008) 3459-3464.
[42] W.-C. Hou, C.T. Jafvert, Photochemical Transformation of Aqueous C_{60} Clusters in Sunlight, Environmental Science & Technology 43(2) (2008) 362-367.
[43] W.-C. Hou, C.T. Jafvert, Photochemistry of aqueous C_{60} clusters: evidence of $^1O_2$ formation and its role in mediating C_{60} phototransformation, Environmental science & technology 43(14) (2009) 5257-5262.
[44] W.-C. Hou, L. Kong, K.A. Wepasnick, R.G. Zepp, D.H. Fairbrother, C.T. Jafvert, Photochemistry of Aqueous C60 Clusters: Wavelength Dependency and Product Characterization, Environmental Science & Technology 44(21) (2010) 8121-8127.
[45] C. Taliani, G. Ruani, R. Zamboni, R. Danieli, S. Rossini, V. Denisov, V. Burlakov, F. Negri, G. Orlandi, F. Zerbetto, Light-induced oxygen incision of C60, Journal of the Chemical Society, Chemical Communications (3) (1993) 220-222.
[46] R. Gelca, K. Surowiec, T.A. Anderson, S.B. Cox, Photolytic breakdown of fullerene C60 cages in an aqueous suspension, Journal of nanoscience and nanotechnology 11(2) (2011) 1225-1229.
[47] D. Heymann, S.M. Bachilo, R.B. Weisman, F. Cataldo, R.H. Fokkens, N.M.M. Nibbering, R.D. Vis, L.P.F. Chibante, C60O3, a Fullerene Ozonide: Synthesis and Dissociation to C60O and O2, Journal of the American Chemical Society 122(46) (2000) 11473-11479.
[48] B.S. Murdianti, J.T. Damron, M.E. Hilburn, R.D. Maples, R.S. Hikkaduwa Koralege, S.I. Kuriyavar, K.D. Ausman, C60 oxide as a key component of aqueous C60 colloidal suspensions, Environmental science & technology 46(14) (2012) 7446-7453.
[49] A.J. Tiwari, J.R. Morris, E.P. Vejerano, M.F. Hochella Jr, L.C. Marr, Oxidation of C_{60} aerosols by atmospherically relevant levels of O_3, Environmental science & technology 48(5) (2014) 2706-2714.
[50] A. Carboni, R. Helmus, J.R. Parsons, K. Kalbitz, P. de Voogt, Incubation of solid state C 60 fullerene under UV irradiation mimicking environmentally relevant conditions, Chemosphere 175 (2017) 1-7.
[51] H. Mashayekhi, S. Ghosh, P. Du, B. Xing, Effect of natural organic matter on aggregation behavior of C60 fullerene in water, Journal of Colloid and Interface Science 374(1) (2012) 111-117.

[52] K.L. Chen, M. Elimelech, Interaction of Fullerene (C60) Nanoparticles with Humic Acid and Alginate Coated Silica Surfaces: Measurements, Mechanisms, and Environmental Implications, Environmental Science & Technology 42(20) (2008) 7607-7614.
[53] D.R. Kester, I.W. Duedall, D.N. Connors, R.M. Pytkowicz, Preparation of artificial seawater, Limnol. Oceanogr 12(1) (1967) 176-179.
[54] D.L. Lipschitz, W.C. Michel, Amino acid odorants stimulate microvillar sensory neurons, Chemical senses 27(3) (2002) 277-286.
[55] A. Hirsch, The chemistry of the fullerenes, Wiley Online Library1994.
[56] Y. Elemes, S.K. Silverman, C. Sheu, M. Kao, C.S. Foote, M.M. Alvarez, R.L. Whetten, Reaction of C60 with Dimethyldioxirane—Formation of an Epoxide and a 1, 3-Dioxolane Derivative, Angewandte Chemie International Edition in English 31(3) (1992) 351-353.
[57] S. Patai, The chemistry of peroxides, John Wiley & Sons2015.
[58] R. Dattani, K.F. Gibson, S. Few, A.J. Borg, P.A. DiMaggio, J. Nelson, S.G. Kazarian, J.T. Cabral, Fullerene oxidation and clustering in solution induced by light, Journal of colloid and interface science 446 (2015) 24-30.
[59] A.L. Balch, D.A. Costa, B.C. Noll, M.M. Olmstead, Oxidation of buckminsterfullerene with m-chloroperoxybenzoic acid. Characterization of a Cs isomer of the diepoxide C60O2, Journal of the American Chemical Society 117(35) (1995) 8926-8932.
[60] Y. Tajima, K. Takeshi, Y. Shigemitsu, Y. Numata, Chemistry of fullerene epoxides: Synthesis, structure, and nucleophilic substitution-addition reactivity, Molecules 17(6) (2012) 6395-6414.
[61] J.-P. Deng, C.-Y. Mou, C.-C. Han, Electrospray and laser desorption ionization studies of C60O and isomers of C60O2, The Journal of Physical Chemistry 99(41) (1995) 14907-14910.
[62] J. Feng, A. Ren, W. Tian, M. Ge, Z. Li, C. Sun, X. Zheng, M.C. Zerner, Theoretical studies on the structure and electronic spectra of some isomeric fullerene derivatives C60On (n= 2, 3), International Journal of Quantum Chemistry 76(1) (2000) 23-43.
[63] D. Heymann, S.M. Bachilo, R.B. Weisman, F. Cataldo, R.H. Fokkens, N.M. Nibbering, R.D. Vis, L.F. Chibante, C60O3, a fullerene ozonide: synthesis and dissociation to C60O and O2, Journal of the American Chemical Society 122(46) (2000) 11473-11479.
[64] Y. Tajima, K. Takeuchi, Discovery of C60O3 Isomer Having C 3v Symmetry, The Journal of organic chemistry 67(5) (2002) 1696-1698.
[65] M. Manoharan, Predicting efficient C60 epoxidation and viable multiple oxide formation by theoretical study, The Journal of organic chemistry 65(4) (2000) 1093-1098.
[66] R. Bulgakov, E.Y. Nevyadovskii, A. Belyaeva, M. Golikova, Z. Ushakova, Y.G. Ponomareva, U. Dzhemilev, S. Razumovskii, F. Valyamova, Water-soluble polyketones and esters as the main stable products of ozonolysis of fullerene C60 solutions, Russian chemical bulletin 53(1) (2004) 148-159.
[67] N. Xin, X. Yang, Z. Zhou, J. Zhang, S. Zhang, L. Gan, Synthesis of C60 (O) 3: An open-cage fullerene with a ketolactone moiety on the orifice, The Journal of organic chemistry 78(3) (2013) 1157-1162.
[68] S. Lebedkin, S. Ballenweg, J. Gross, R. Taylor, W. Krätschmer, Synthesis of $C_{120}O$: A new dimeric [60] fullerene derivative, Tetrahedron letters 36(28) (1995) 4971-4974.
[69] A. Gromov, S. Lebedkin, S. Ballenweg, A.G. Avent, R. Taylor, W. Krätschmer, $C_{120}O_2$: The first [60] fullerene dimer with cages bis-linked by furanoid bridges, Chemical Communications (2) (1997) 209-210.
[70] R. Taylor, M.P. Barrow, T. Drewello, C 60 degrades to C 120 O, Chemical Communications (22) (1998) 2497-2498.

[71] M. Silion, A. Dascalu, M. Pinteala, B.C. Simionescu, C. Ungurenasu, A study on electrospray mass spectrometry of fullerenol $C_{60}(OH)_{24}$, Beilstein journal of organic chemistry 9(1) (2013) 1285-1295.
[72] J. Labille, A. Masion, F. Ziarelli, J. Rose, J. Brant, F. Villiéras, M. Pelletier, D. Borschneck, M.R. Wiesner, J.-Y. Bottero, Hydration and Dispersion of C60 in Aqueous Systems: The Nature of Water−Fullerene Interactions, Langmuir 25(19) (2009) 11232-11235.
[73] Y.S. Hwang, Q. Li, Characterizing Photochemical Transformation of Aqueous nC_{60} under Environmentally Relevant Conditions, Environmental Science & Technology 44(8) (2010) 3008-3013.
[74] J. Brant, H. Lecoanet, M.R. Wiesner, Aggregation and Deposition Characteristics of Fullerene Nanoparticles in Aqueous Systems, Journal of Nanoparticle Research 7(4) (2005) 545-553.
[75] X. Qu, P.J. Alvarez, Q. Li, Impact of sunlight and humic acid on the deposition kinetics of aqueous fullerene nanoparticles (nC60), Environmental science & technology 46(24) (2012) 13455-13462.
[76] K. Polewski, D. Sławińska, J. Sławiński, A. Pawlak, The effect of UV and visible light radiation on natural humic acid: EPR spectral and kinetic studies, Geoderma 126(3–4) (2005) 291-299.
[77] M. Kah, X. Zhang, T. Hofmann, Sorption behavior of carbon nanotubes: Changes induced by functionalization, sonication and natural organic matter, Science of The Total Environment 497-498(0) (2014) 133-138.
[78] H.S. Thorsten Hüffer, Melanie Kah, Thilo Hofmann, Sorption of substituted aromatic hydrocarbons by fullerenes - Influence of functionalization on molecular interactions, Poster presentation at the SETAC Europe 26th Annual Meeting (Nantes, France, 2016) (2016).
[79] K. Gai, B. Shi, X. Yan, D. Wang, Effect of dispersion on adsorption of atrazine by aqueous suspensions of fullerenes, Environmental science & technology 45(14) (2011) 5959-5965.
[80] T. Hüffer, M. Kah, T. Hofmann, T.C. Schmidt, How redox conditions and irradiation affect sorption of PAHs by dispersed fullerenes (nC60), Environmental science & technology 47(13) (2013) 6935-6942.
[81] T.D. Berry, A.P. Clavijo, Y. Zhao, C.T. Jafvert, R.F. Turco, T.R. Filley, Soil microbial response to photo-degraded C60 fullerenes, Environmental Pollution 211 (2016) 338-345.
[82] T.M. Sakellarides, M.G. Siskos, T.A. Albanis, Photodegradation of selected organophosphorus insecticides under sunlight in different natural waters and soils, International Journal of Environmental & Analytical Chemistry 83(1) (2003) 33-50.

SUPPLEMENTARY INFORMATION

Transformation of C_{60} fullerene aggregates suspended and weathered under realistic environmental conditions

Josep Sanchís[1,†], Yann Aminot[2,†], Esteban Abad[1], Damià Barceló[1,3], James W. Readman[2], Marinella Farré[1,*]

[1] Water and Soil Quality Research Group, Institute of Environmental Assessment and Water Research (IDAEA-CSIC), C/Jordi Girona, 18-26, 08034, Barcelona, Catalonia, Spain.
[2] Plymouth University, Plymouth, England, UK.
[3] Catalan Institute of Water Research (ICRA), C/ Emili Grahit, 101, 17003 Girona, Catalonia, Spain.

[†] Both authors contributed equally to this work.

[*] *Corresponding author*: mfuqam@cid.csic.es

Text S1. Extraction optimization

Optimization: A simple one-step liquid-liquid extraction method was optimized. Three C_{60} suspensions were prepared at ~1.0 mg l^{-1} in three different water matrices (UPW, AFW and ASW) and weathered under ambient sunlight irradiation during 24 h with constant stirring. Five extraction solvents were tested: toluene, *o*-dichlorobenzene, ethyl acetate, dichloromethane and the water-insoluble ionic liquid [BMIM][PF_6].

Results: Based on the amount of C_{60} and $C_{60}O_2$ recovered, the performance of the tested solvents ranked as follows: toluene > *o*-dichlorobenzene > dichloromethane > ethyl acetate > [BMIM][PF_6] (see **Figure S1**). Toluene was the optimal extraction solvent. The three non-aromatic compounds (the ionic liquid, dichloromethane and ethyl acetate) showed the lowest recovery yields, always lower than 4 %. In addition, the peak shape worsened significantly when injecting dichloromethane and [BMIM][PF_6] extracts, probably because of the low diffusion of these solvents into the mobile phase. On the contrary, *o*-dichlorobenzene and, especially, toluene, offered good recoveries.

In addition, as can be seen in **Figure S1**, the extraction recovery was slightly dependent on the ionic strength of the matrix, as it has been reported in other works which recommend salting out the water sample to optimize the extraction of fullerenes [1].

Text S2: Chromatographic optimization

The formation of fullerene adducts was first reported by van Wezel *et al*. (2011) [2]. The simultaneous analysis of fullerene C_{60} and their transformation products is challenging because oxygenated adducts produce signals with the same m/z than the molecular ions of degradation products generated under environmental conditions. In addition, $C_{60}O_x$ molecules are fragmented in the ionisation source losing oxygen atoms. Therefore, C_{60} and their oxidized transformation products have a common series of isobaric signals that can potentially interfere with each other if they are not correctly separated by the chromatographic step (see **Table S1**).

A toluene extract of C_{60}, suspended in UPW and weathered as described in **Text S1**, was used for the chromatographic optimisation. The separation between the parent C_{60} fullerene and the generated transformation products $C_{60}O$ and $C_{60}O_2$ was optimised.

Four LC columns were tested:

- A Luna® C18 column (length, 15.0 cm; diameter, 2 mm; particle size, 5 µm; pore size, 100 Å) from Phenomenex, Torrance, CA, USA;
- a HILIC column (length, 15.0 cm; diameter, 2 mm; particle size, 3 µm; pore size, 200 Å) from Phenomenex, Torrance, CA, USA;
- a Cosmosil Buckyprep D column (length, 15.0 cm; diameter, 2 mm; particle size, 5 µm; pore size, ~120 Å) from Nacalai Tesque Inc., Kyoto, Japan; and
- a Cosmosil Buckyprep column (length, 15.0 cm; diameter, 2 mm; particle size, 5 µm; pore size, ~120 Å) from Nacalai Tesque Inc., Kyoto, Japan.

Tests with C18 columns using isocratic mobile phases consisting in toluene:methanol (1:1) and toluene:acetonitrile (1:1) showed no separation of these three peaks. Therefore, other columns were tested.

A Luna® HILIC column was also tested. Early tests with H_2O:MeOH and H_2O:ACN gradients were inadequate, since toluene is mandatory for the elution of fullerenes and their oxidized derivatives. Toluene was introduced in tertiary mobile phases of methanol:water:toluene (ratios of 80:15:5, 80:10:10 and 80:5:15). Poor results were obtained because of the high retention of fullerene to the column in these conditions.

Non-aqueous HILIC chromatography was employed using methanol and toluene as mobile phases at ratios close to 1:1. Although these conditions offered gaussian peaks with adequate

retention factors (k'≈3, similarly than with conventional non-aqueous reverse phase chromatography with C18 columns), the three compounds, C_{60}, $C_{60}O$ and $C_{60}O_2$, could not be separated.

The performance of two columns especially designed for the separation of fullerenes was assessed: A Cosmosil Buckyprep D and a Cosmosil Buckyprep column, with nitrocarbazoyl and pyrenylpropyl groups respectively.

The Cosmosil Buckyprep D column contains a stationary phases end-capped with nitrocarbazoyl groups, especially indicated for the retention of fullerenes with engineered functional group. Isocratic chromatographic programs were tested with toluene:methanol and toluene:hexane at solvent ratios 100:0, 90:10, 80:20, 70:30 and 60:40. In tests with toluene:methanol, when increasing the amount of methanol, the retention time of the compounds decreased and so did their retention factor, from $k'(C_{60})$=0.29 and $k'(C_{60}O_2)$=0.99 at 100 % of toluene to $k'(C_{60})$=0.01 and $k'(C_{60}O_2)$=0.15 at 40 % of methanol. In tests with toluene:hexane, the opposite trend was observed and the retention increased when increasing the percentage of hexane. The retention of the analytes increased up to $k'(C_{60})$=0.96 and $k'(C_{60}O_2)$=2.9 at 40 % of hexane.

Despite of the good retention and of the Gaussian shape of the peaks, poor chromatographic selectivity was obtained for C_{60} and $C_{60}O$. Both peaks overlapped in all the tested conditions, with an optimal resolution of only 0.12. In tests with toluene:hexane, $C_{60}O_2$ and $C_{60}O$ showed a better selectivity than in tests with toluene:methanol, but the width of the peaks was too large to ensure good chromatographic resolution (*Rs*): $Rs(C_{60}O,C_{60}O_2)$=0.56 at 20 % of hexane and $Rs(C_{60}O,C_{60}O_2)$=0.68 at 30 % of hexane.

Therefore, it was concluded that Buckyprep-D was not an adequate column for the determination of the oxygenated photodegradation products of C_{60}.

In constrast, the Buckyprep column showed a good performance and it was finally selected as the optimal column. The best chromatographic separation was observed with 10 % of methanol in the mobile phase (see **Figure S2**). At higher percentages of methanol, higher retention factors (k') were observed for all the compounds and the chromatographic selectivity of C_{60}, $C_{60}O$ and $C_{60}O_2$ improved accordingly, but the widening of the peaks and the subsequent loss of sensitivity prevented the use of methanol percentages higher than 10 %. The loss of

sensitivity was related to the widening of the chromatographic peak and to the reduction in ionisation efficiency in the APPI source, as toluene acts as a dopant.

The pH of the mobile phase was modified by adding formic acid contents of 0.01 % and 0.1 % in the methanol. No significant changes were observed in the chromatographic performance, so the mobile phase was not acidified.

Finally, the temperature of the column oven was optimized with better results obtained at T=30 ºC (see **Figure S3**).

Text S3: Mass spectrometry optimization

Preliminary experiments with a heated electrospray (H-ESI) source, an atmospheric pressure chemical ionisation (APCI) source and an APPI source showed that APPI system is the optimal, not only for the analysis of pristine fullerenes (as previously reported [3-5]), but also for ionising the transformation products that were studied in the present work.

High S-lens values favoured the sensitivity of the method, so it was set at 90 % (see **Figure S4**). High temperatures did not favour the ionisation of the compounds, so the capillary temperature was kept at 300 ºC and the probe was adjusted at 400 C. Finally, intermediate gas flows, i.e. sheath gas=40 a.u. and auxiliary gas=25 a.u, were the optimal ones. The spare gas was maintained at 1 a.u. in all the experiments.

In these conditions, the ionisation of C_{60} fullerene resulted in several relevant source adducts. Their identity and relative intensities are listed in **Table S2**.

Text S4: Precautions and safety considerations

During samples manipulation and extraction their exposure to ambient air and light was minimized to avoid undesired and uncontrolled degradation of nC_{60}. Toluene extracts were analysed immediately when possible or stored in amber glass vials at -80 ºC until their instrumental analysis, within 12 hours.

Plastic material was avoided during the whole experimental work in order to avoid adsorption of fullerene aggregates. Instead, glass, quartz and steel instrumentation was employed. Potential carry-over and cross-contamination were circumvented by rinsing glass and quartz material, before and after using it, with toluene, ethanol and acetone. Glass and quartz material was heated at 400 ºC overnight.

In order to minimize health risks, samples extraction and manipulation of organic solvents was carried out under extracting fume. The LC-MS system was installed inside a home-made extracting cabin in order to avoid analysts' exposure to toluene vapour from the chromatographic system and the ionisation source.

Text S5. Data treatment: necessity to normalize by the concentration of C_{60} in each time.

A general scheme of all the processes that happened simultaneously during the stirring and weathering of the aggregates is presented in **Figure S9**, considering (i) those non-suspended aggregates that are present in the air-water interphase, referred to as $(C_{60})_{suspended}$ and $(TP)_{suspended}$; (ii) the truly suspended aggregates that are present in the bulk solution, referred to as $(C_{60})_{suspended}$ and $(TP)_{suspended}$; and (iii) those aggregates that have precipitated or were stuck on the glass walls, referred to as $(C_{60})_{precip}$ and $(TP)_{precip}$. The following assumptions were made:

- Since the degradation experiments were under a constant agitation, $k_{prep.1}$ and k_{prep2} were considered negligible. Subsequently, k_3 was irrelevant and [$(C_{60})_{precip}$] and [$(TP)_{precip}$] could be considered negligible.
- Since the concentration of the other species involved in the reactions (presumably $^1O_2$, O_3, and H_2O) was significantly higher than that of C_{60} and their degradation products, their concentrations could be considered constant and k_1 and k_2 could be considered equivalent (k_{degrad}).
- Since C_{60} fullerene and their transformation products were expected to aggregate together, k_{susp1} and k_{susp2} were assumed to be equivalent (k_{susp}). k_{susp} was not necessarily constant through the reaction, since the solubility of the aggregate increases accordingly with the concentration of oxidized transformation products.

The aliquots analysed by LC-MS were taken from the bulk solution, so only $(C_{60})_{suspended}$ and $(TP)_{suspended}$ were analysed. Both were decisively affected by k_{sup}, so in order to study the kinetics of degradation circumventing the interference of the kinetic of solubilisation, the concentrations of transformation products were normalised by the concentration of C_{60} fullerene at each sampling point. This concentration of C_{60} in the bulk solution evolved through time in a non-trivial way and the maximum concentration of C_{60} was usually obtained after 12 h~24 h.

Table S1. Intensity of oxygen adducts and "fullerene-like" in-source fragments, normalised by the intensity of the molecular radical ion (in bold).

	$[C_{60}]^{\cdot -}$	$[C_{60}O]^{\cdot -}$	$[C_{60}O_2]^{\cdot -}$	$[C_{60}O_3]^{\cdot -}$	$[C_{60}O_4]^{\cdot -}$
	m/z=720.0005	m/z=735.9954	m/z=751.9904	m/z=767.9852	m/z=783.9802
C_{60}	**1.0**	0.019	0.0005	0.0002	<0.0001
$C_{60}O$ (*k'*=3.0)	4.1	**1.0**	0.02	0.01	<0.0001
$C_{60}O_2$ (*k'*=3.8)	2.1	0.13	**1.0**	0.07	0.06

Table S2. List of adducts and their relative intensities, obtained when analysing a fresh standard of C_{60} fullerene in the optimal MS conditions. Experimental m/z presented an error smaller than 1.5 ppm in all the cases.

	m/z	Adduct	Intensity (%)	Comment
1	721.0084	$[C_{60}\ H]^{\cdot -}$	3.5	Proton adduct. Has overlapping with the $[^{12}C_{59}\ ^{13}C]^{\cdot -}$ signal.
2	735.9954	$[C_{60}\ O]^{\cdot -}$	1.9	Monoxidized adduct.
3	737.0033	$[C_{60}\ OH]^{\cdot -}$	0.47	Hydroxyl adduct. Has overlapping with the $[^{12}C_{59}\ ^{13}C\ O]^{\cdot -}$ signal.
4	738.0111	$[C_{60}\ OH_2]^{\cdot -}$	0.093	Water adduct (or C_{60}+OH+H adduct). Has overlapping with the $[^{12}C_{59}\ ^{13}C\ OH]^{\cdot -}$ signal.
5	751.9904	$[C_{60}\ O_2]^{\cdot -}$	0.050	Dioxidized adduct.
6	752.9982	$[C_{60}\ O_2H]^{\cdot -}$	0.75	Overlapping with the $[^{12}C_{59}\ ^{13}C\ O_2]^{\cdot -}$ signal.
7	767.9852	$[C_{60}\ O_3]^{\cdot -}$	0.017	Three-fold-oxidized adduct.
8	812.0631	$[C_{60}\ C_7H_8]^{\cdot -}$	2.5	Toluene adduct (from the mobile phase)
9	751.0189	$[C_{60}\ OCH_3]^{\cdot -}$	0.021	Methanol adduct (from the mobile phase).
10	844.0893	$[C_{60}\ C_7H_8\ CH_3OH]^{\cdot -}$	0.24	Toluene and methanol adduct (from the mobile phase)
11	720.5022	$[C_{60}\ C_{60}]^{\cdot 2-}$	0.0054	Dimer, only observed with double charge.
12	720.3350	$[C_{60}\ C_{60}\ C_{60}]^{\cdot 3-}$	0.0012	Trimer, only observed with triple charge.

Figure S1. Extraction of C_{60} and $C_{60}O_2$ with the different tested solvents in the three studied matrixes: ultrapure water, artificial freshwater and artificial seawater.

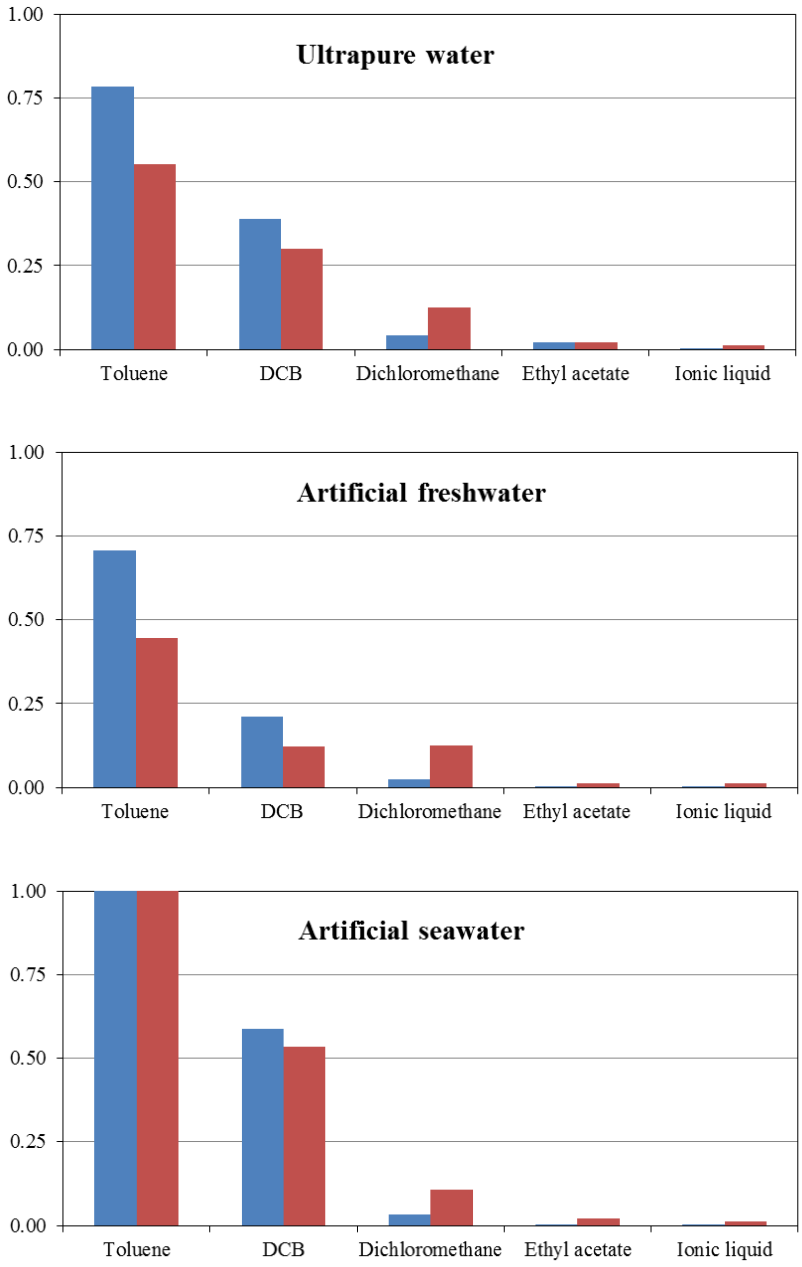

Figure S2. Separation of C_{60}, $C_{60}O$ and $C_{60}O_2$ in a Buckyprep column, using isocratic mobile phases containing 0 %, 10 % and 20 % of methanol.

	Toluene	**Toluene:methanol 90:10**	**Toluene:methanol 80:20**
$[C_{60}]^{\cdot -}$ (m/z=720.0005±0.0001)	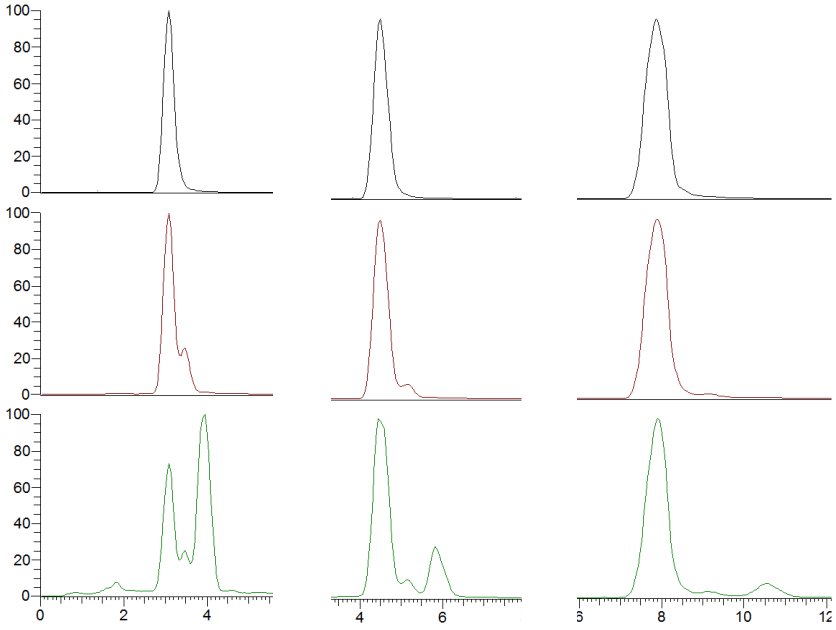		
$[C_{60}O]^{\cdot -}$ (m/z=735.9954±0.0001)			
$[C_{60}O_2]^{\cdot -}$ (m/z=751.9904±0.0001)			

Figure S3. Extracted ion chromatograms (m/z=720.0005±0.0001) showing the chromatographic peaks of C_{60} and its transformation product $C_{60}O$ in a toluene extract. Chromatographic separation was achieved in a Buckyprep column, using toluene:methanol (90:10) as mobile phase at different temperatures (25 ºC, 30 ºC, 35 ºC and 40 ºC).

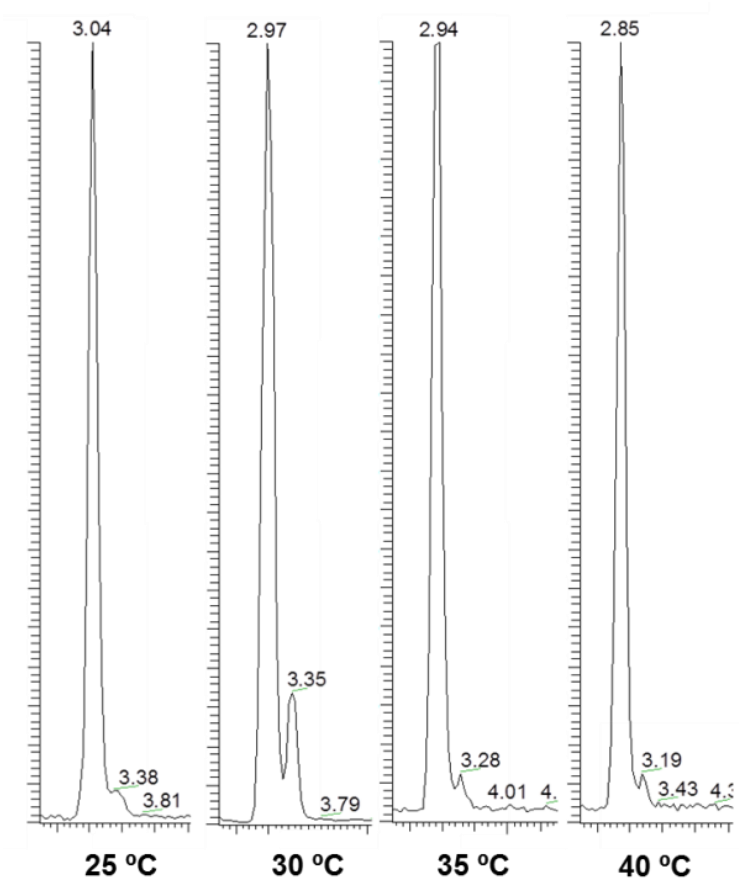

Figure S4. Normalised intensities of the $[C_{60}]^{\cdot -}$ radical ion when working at different APPI conditions. Relatively low source temperatures, intermediate gas flows and high S-lens RF levels resulted in the optimal performance.

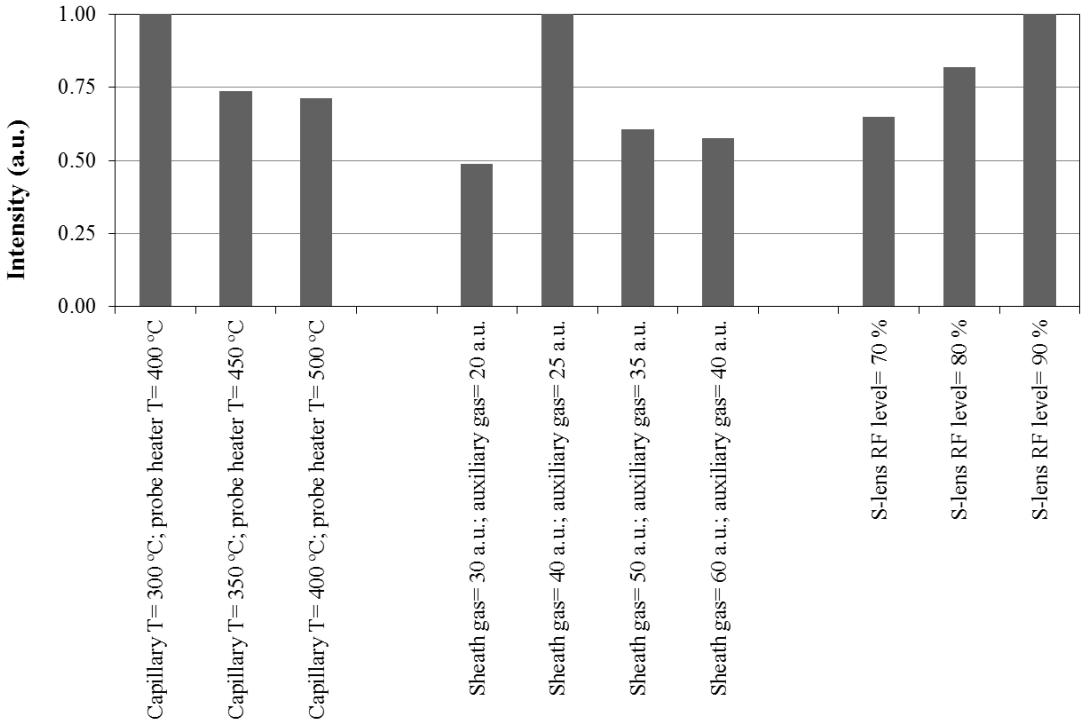

Figure S5. Structures of the two molecules with formula $C_{60}O$. *a*: C_{60} epoxide ([6,6]$C_{60}O$); *b*: C_{60} oxidoannulene ([5,6]$C_{60}O$).

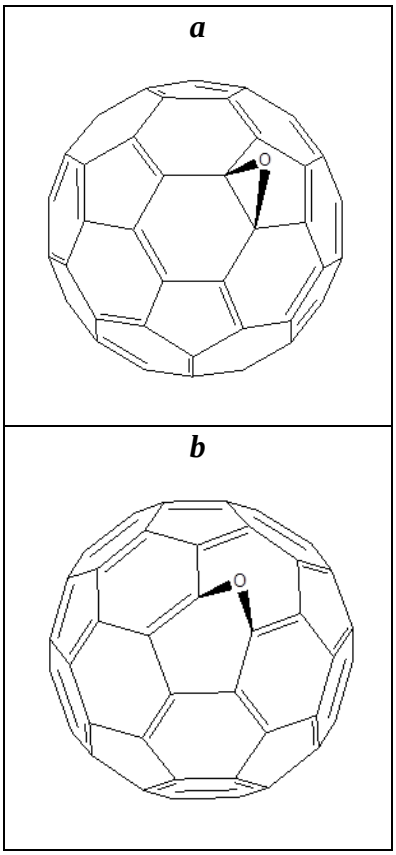

Figure S6. Structures of selected regioisomers of triepoxidized C_{60} fullerenes (*a*, *b* and *c*).

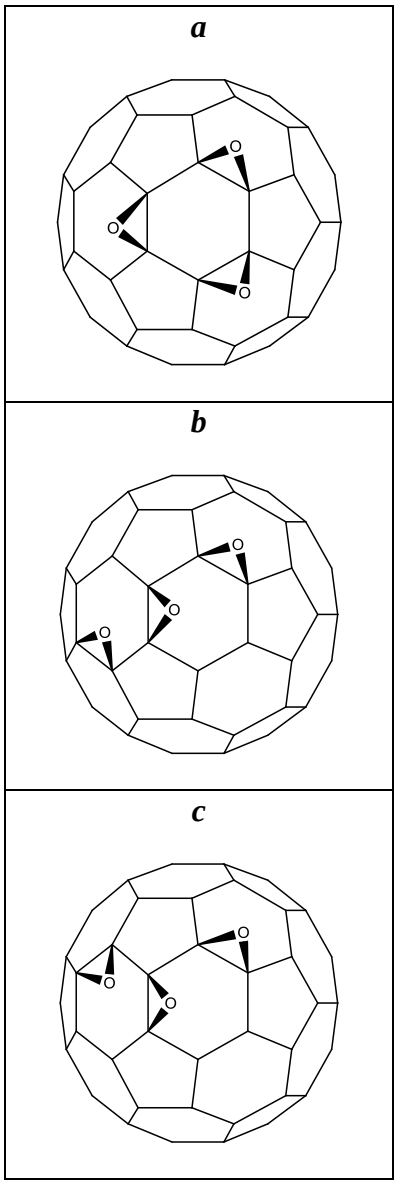

Figure S7. Structure of the most stable tetraepoxidized C_{60} fullerene.

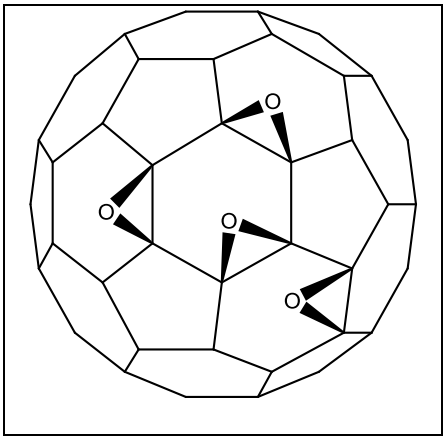

Figure S8. Signals of fullerenols observed in suspensions after sonication. Figure *a* shows a total ion chromatogram with three principal groups of signals: the peak of C_{60} fullerene (t_R=3.00), a peak of overlapped fullerenols at (t_R=1.84) and unretained peaks near the dead volume (t_R=1.01). The extracted ion chromatograms of $[C_{60}O]\cdot^-$, $[C_{60}O_2H]\cdot^-$ and $[C_{60}O_6H_5]\cdot^-$ are shown in Figure *b*, *c* and *d*.

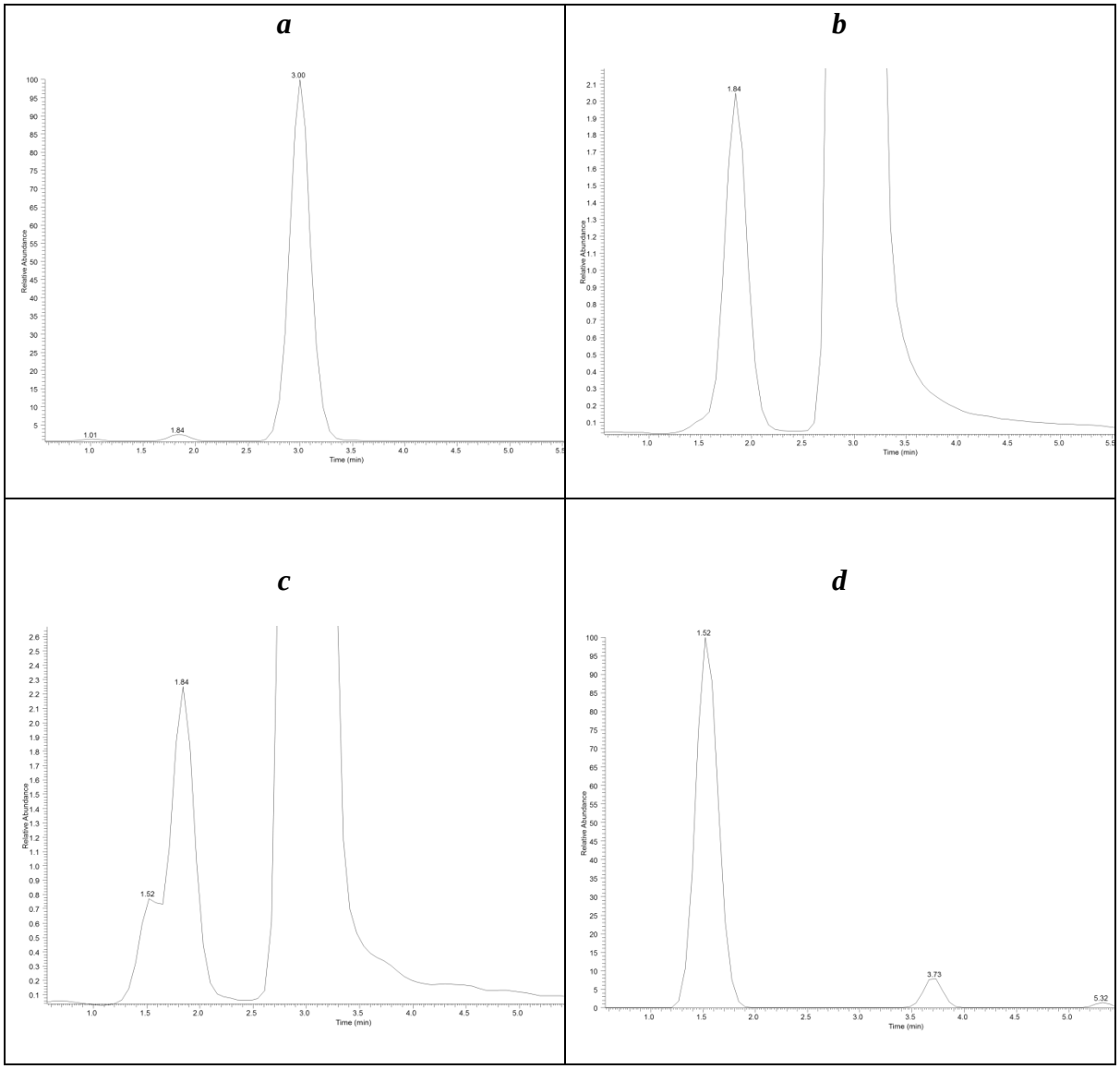

Figure S9. General scheme of reactions happening in the system.

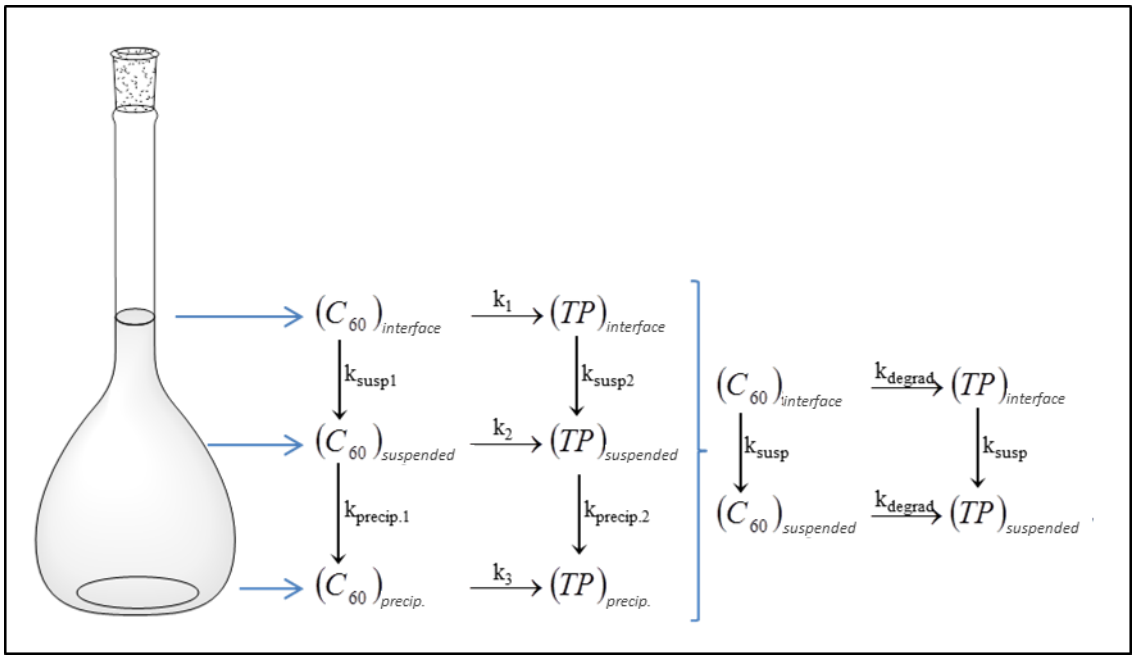

Figure S10. Generation and degradation of $C_{120}O$ and $C_{120}O_2$ in ultrapure water

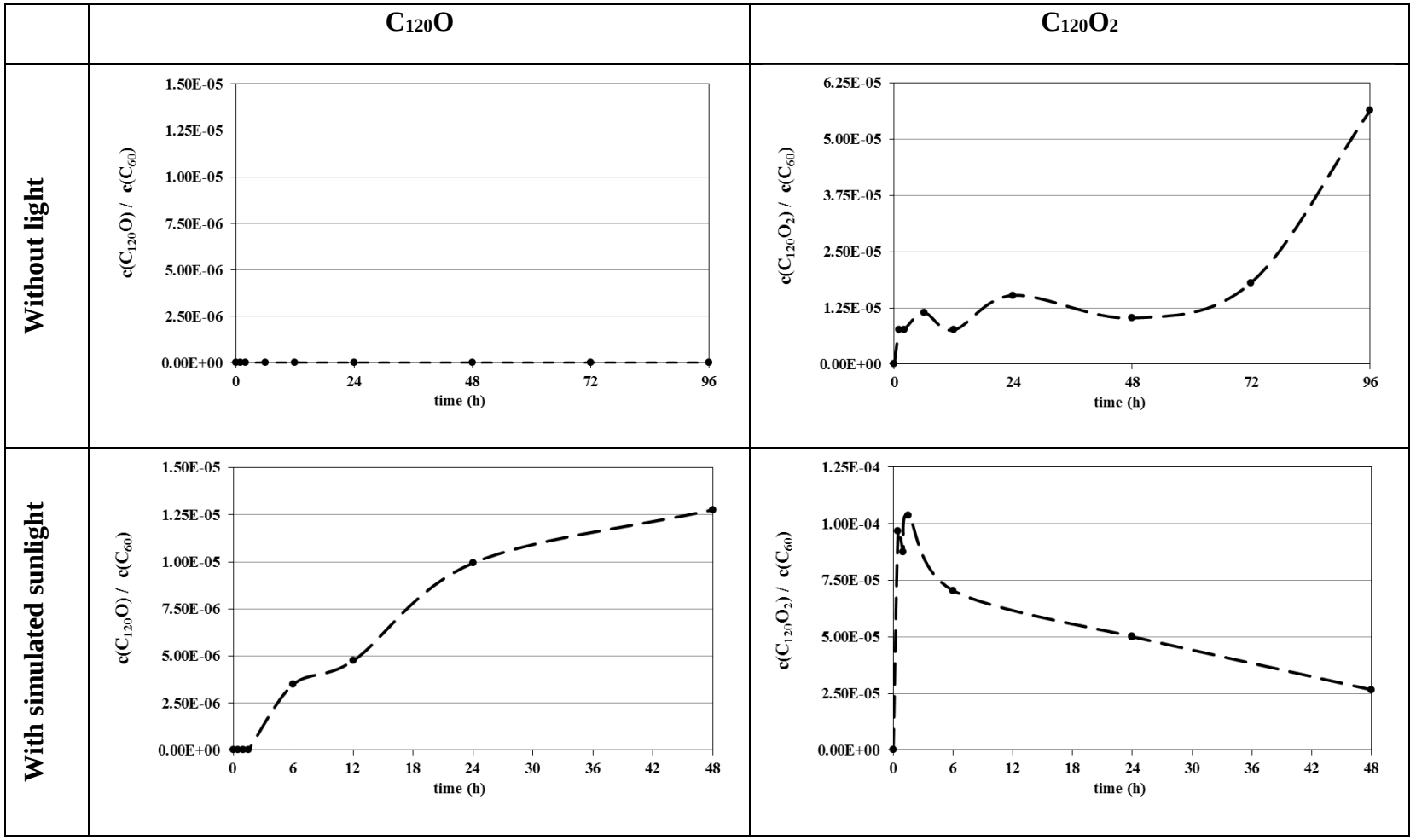

Figure S11. Impact of salinity (● = 5.8 µS cm^{-1}; ● = 970 µS cm^{-1}; ● = 46,000 µS cm^{-1}) on the generation of selected $C_{60}O_x$.

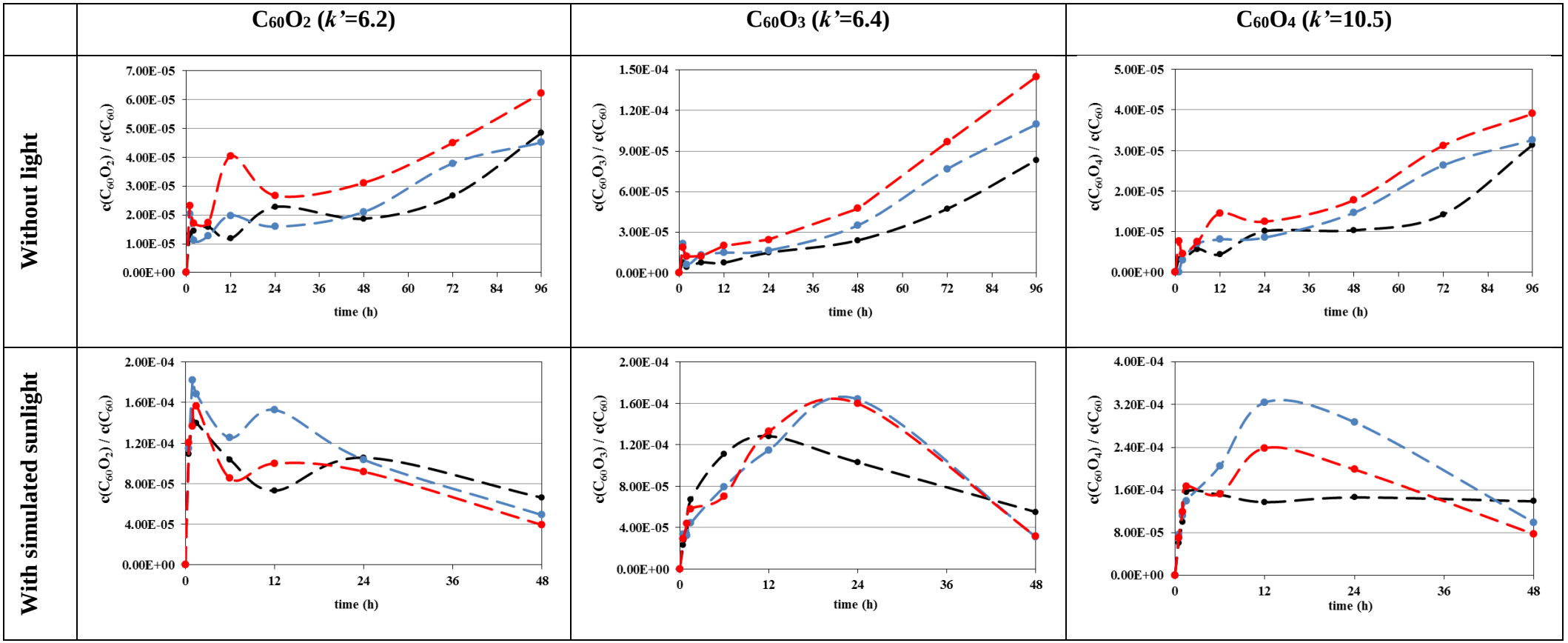

Figure S11 (cont). Impact of salinity (● = 5.8 µS cm^{-1}; ● = 970 µS cm^{-1}; ● = 46,000 µS cm^{-1}) on the generation of selected $C_{120}O_x$.

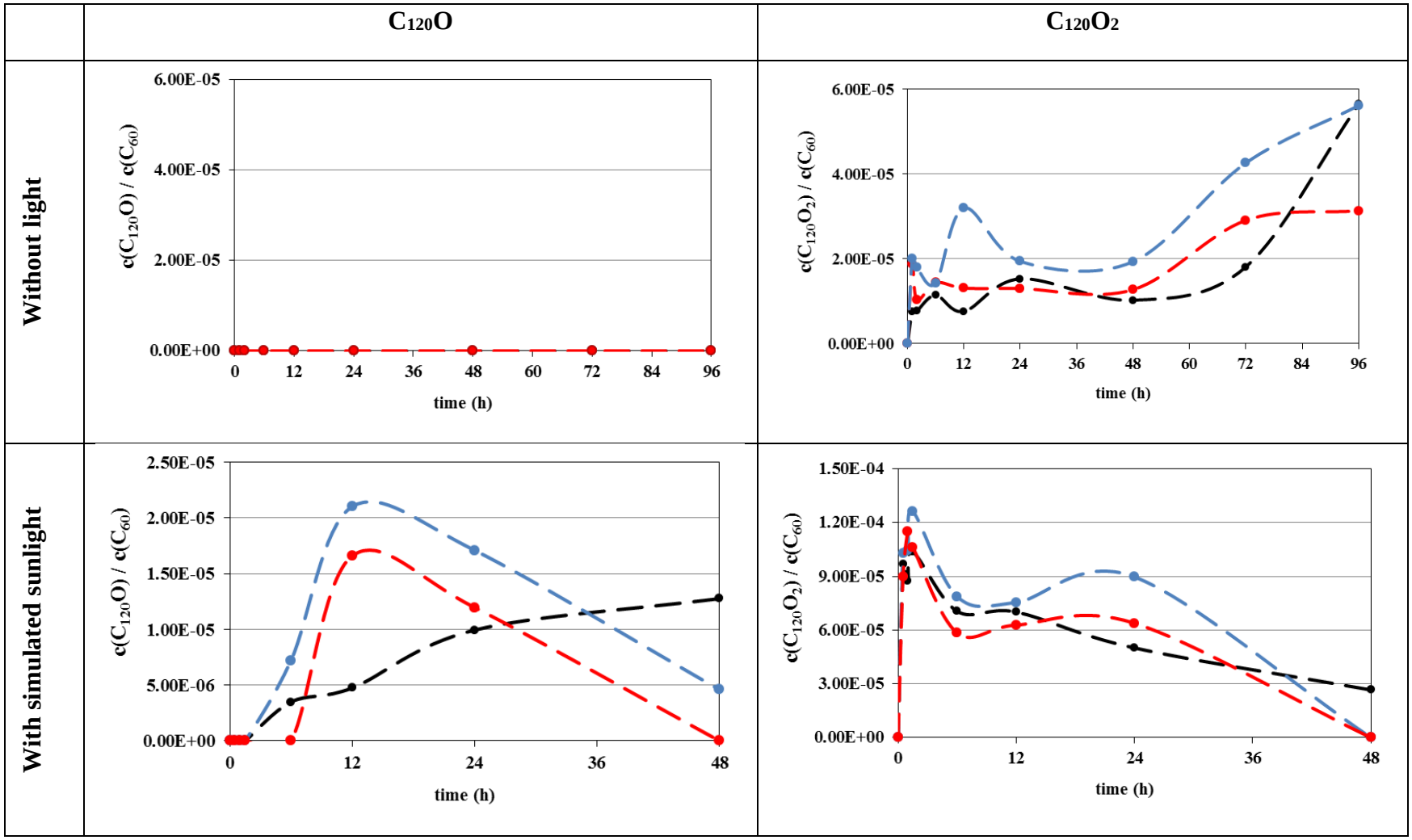

Figure S12. Impact of the pH (●: pH=6.00; ●: pH=7.00; ●: pH=8.15) on the generation of selected $C_{60}O_x$.

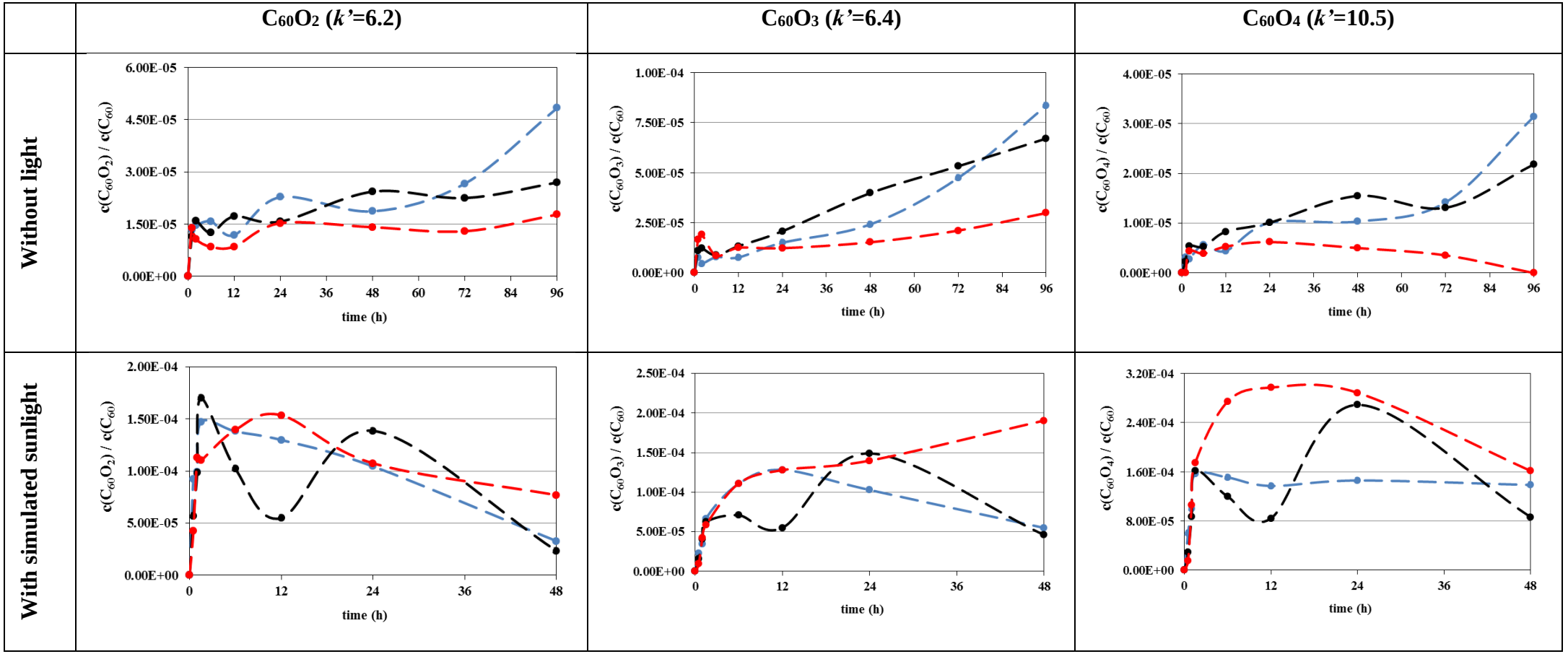

Figure S12(cont). Impact of the pH (●: pH=6.00; ●: pH=7.00; ●: pH=8.15) on the generation of selected $C_{120}O_x$.

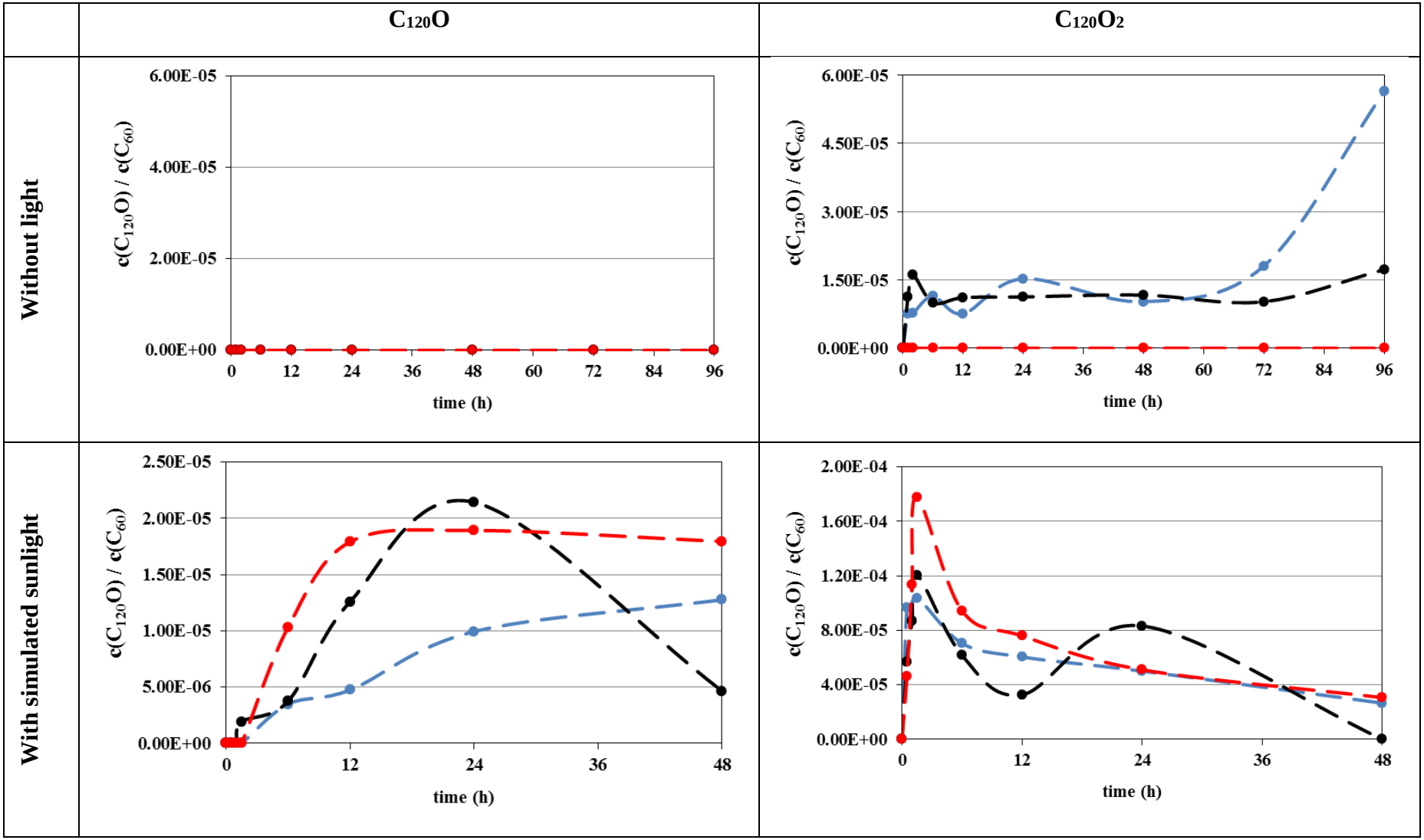

Figure S13. Impact of the humic acids content (●: [HA] = 0 mg l^{-1}; ●: [HA] = 2.25 mg l^{-1}; ●: [HA] = 0.30 mg l^{-1}) on the generation of selected $C_{60}O_x$.

	$C_{60}O_2$ (*k'*=6.2)	$C_{60}O_3$ (*k'*=6.4)	$C_{60}O_4$ (*k'*=10.5)
Without light	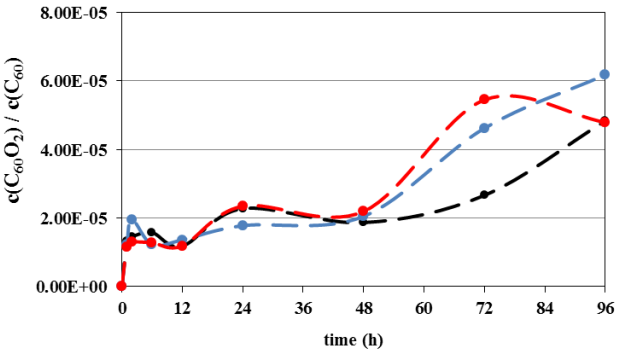	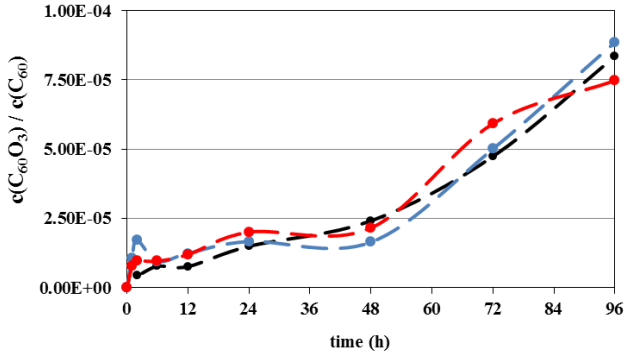	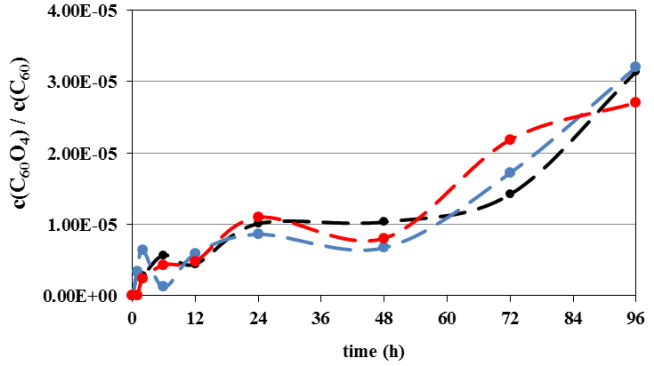
With simulated sunlight	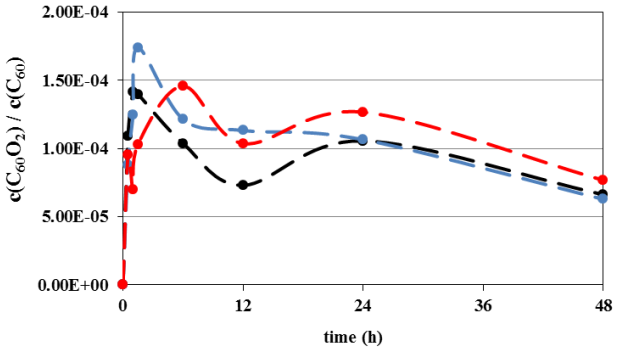	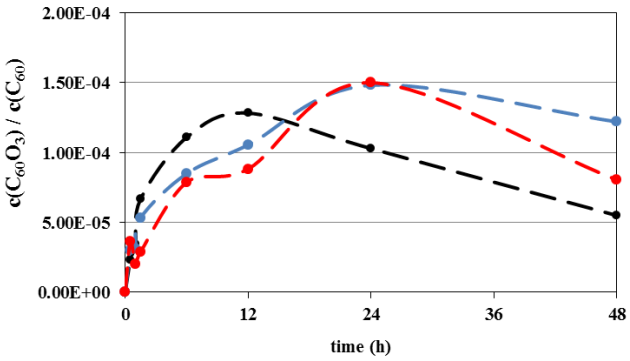	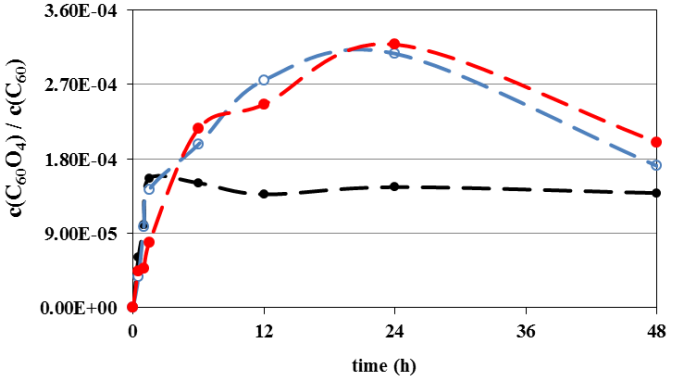

Figure S13 (cont). Impact of the humic acids content (●: [HA] = 0 mg l^{-1}; ●: [HA] = 2.25 mg l^{-1}; ●: [HA] = 0.30 mg l^{-1}) on the generation of selected $C_{120}O_x$.

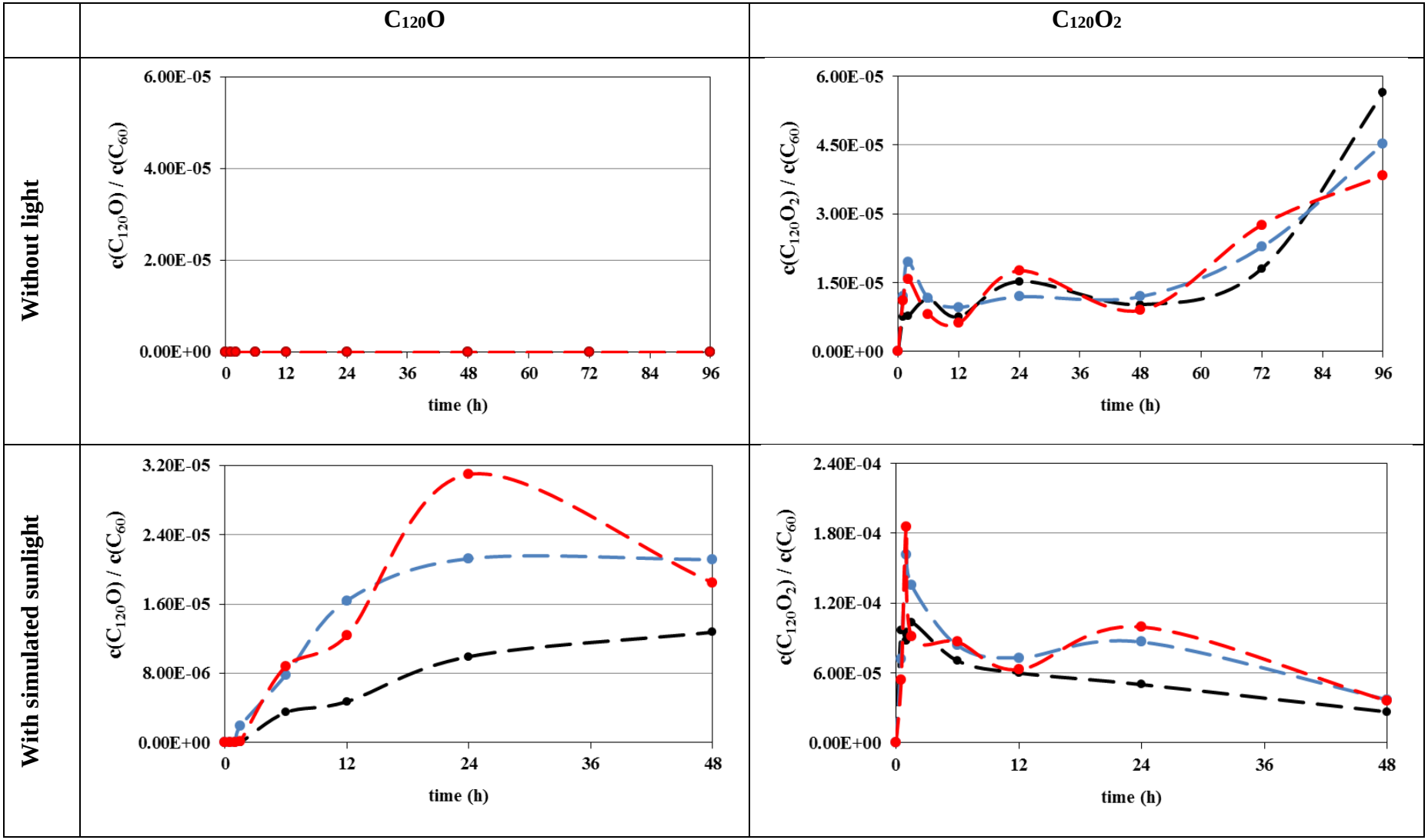

Figure S14. $C_{60}O$ signal in the extract of freshwater from the Besòs River (Barcelona). The first peak belongs to the oxidized adduct of the C_{60} molecule, while the second peak belongs to the tentatively identified transformation product.

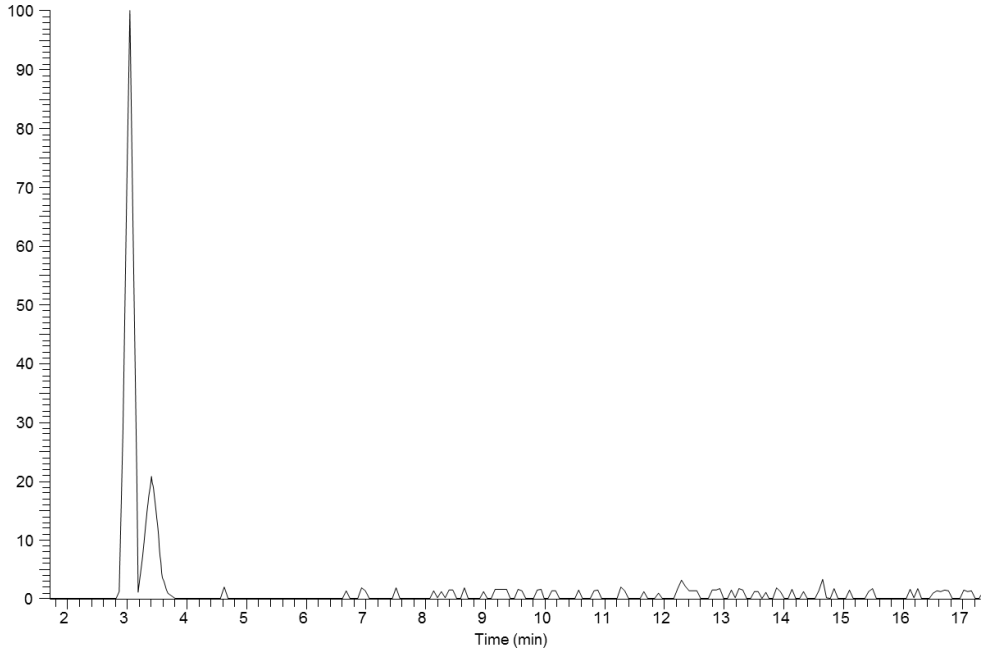

References

[1] D. Bouchard, X. Ma, Extraction and high-performance liquid chromatographic analysis of C60, C70, and [6,6]-phenyl C61-butyric acid methyl ester in synthetic and natural waters, Journal of Chromatography A 1203(2) (2008) 153-159.
[2] A.P. van Wezel, V. Morinière, E. Emke, T. ter Laak, A.C. Hogenboom, Quantifying summed fullerene nC60 and related transformation products in water using LC LTQ Orbitrap MS and application to environmental samples, Environment International 37(6) (2011) 1063-1067.
[3] Ó. Núñez, H. Gallart-Ayala, C.P.B. Martins, E. Moyano, M.T. Galceran, Atmospheric Pressure Photoionization Mass Spectrometry of Fullerenes, Analytical Chemistry 84(12) (2012) 5316-5326.
[4] J. Sanchís, L.F.S. Oliveira, F.B. de Leão, M. Farré, D. Barceló, Liquid chromatography–atmospheric pressure photoionization–Orbitrap analysis of fullerene aggregates on surface soils and river sediments from Santa Catarina (Brazil), Science of the Total Environment 505 (2015) 172-179.
[5] L. Li, S. Huhtala, M. Sillanpää, P. Sainio, Liquid chromatography-mass spectrometry for C60 fullerene analysis: optimisation and comparison of three ionisation techniques, Analytical and bioanalytical chemistry 403(7) (2012) 1931-1938.